

CONSTANS alters the circadian clock in *Arabidopsis thaliana*

Pedro de los Reyes¹, Gloria Serrano-Bueno^{1,4}, Francisco J. Romero-Campero^{1,2}, He Gao³, Jose M. Romero^{1,4} and Federico Valverde^{1,*}

¹Plant Development Group - Institute for Plant Biochemistry and Photosynthesis, Consejo Superior de Investigaciones Científicas, Universidad de Sevilla, Sevilla, Spain

²Department of Computer Science and Artificial Intelligence, Universidad de Sevilla, Sevilla, Spain

³Department of Plant Developmental Biology, Max Planck Institute for Plant Breeding Research, Cologne, Germany

⁴Department of Plant Biochemistry and Molecular Biology, Universidad de Sevilla, Sevilla, Spain

*Correspondence: Federico Valverde (federico.valverde@ibvf.csic.es)

<https://doi.org/10.1016/j.molp.2024.06.006>

ABSTRACT

Plants are sessile organisms that have acquired highly plastic developmental strategies to adapt to the environment. Among these processes, the floral transition is essential to ensure reproductive success and is finely regulated by several internal and external genetic networks. The photoperiodic pathway, which controls plant response to day length, is one of the most important pathways controlling flowering. In *Arabidopsis* photoperiodic flowering, *CONSTANS* (*CO*) is the central gene activating the expression of the florigen *FLOWERING LOCUS T* (*FT*) in the leaves at the end of a long day. The circadian clock strongly regulates *CO* expression. However, to date, no evidence has been reported regarding a feedback loop from the photoperiod pathway back to the circadian clock. Using transcriptional networks, we have identified relevant network motifs regulating the interplay between the circadian clock and the photoperiod pathway. Gene expression, chromatin immunoprecipitation experiments, and phenotypic analysis allowed us to elucidate the role of *CO* over the circadian clock. Plants with altered *CO* expression showed a different internal clock period, measured by daily leaf rhythmic movements. We showed that *CO* upregulates the expression of key genes related to the circadian clock, such as *CCA1*, *LHY*, *PRR5*, and *GI*, at the end of a long day by binding to specific sites on their promoters. Moreover, a high number of *PRR5*-repressed target genes are upregulated by *CO*, and this could explain the phase transition promoted by *CO*. The *CO*-*PRR5* complex interacts with the bZIP transcription factor *HY5* and helps to localize the complex in the promoters of clock genes. Taken together, our results indicate that there may be a feedback loop in which *CO* communicates back to the circadian clock, providing seasonal information to the circadian system.

Key words: CONSTANS, circadian clock, photoperiod

de los Reyes P., Serrano-Bueno G., Romero-Campero F.J., Gao H., Romero J.M., and Valverde F. (2024). CONSTANS alters the circadian clock in *Arabidopsis thaliana*. *Mol. Plant*. **17**, 1204–1220.

INTRODUCTION

In order to interact with a regularly changing environment, plants have developed a great variety of morphological and physiological responses. The transcriptional programs that control these responses allow plants to respond to external stimuli with a high degree of plasticity throughout their life cycles (De Mendoza et al., 2013). One of the most important decisions in the plant life cycle is flowering, which activates the molecular and metabolic changes that induce the transition from the vegetative to the reproductive growth programs (Andrés and Coupland, 2012; Piñeiro and Jarillo, 2013; Kinoshita and Richter, 2020). This transition is finely regulated by multiple factors since making

this decision at the right moment ensures reproductive and evolutionary success. Thus, plants can recognize seasonal changes by measuring day length (photoperiod), allowing them to adapt to and grow at different latitudes. The photoperiodic pathway is one of the major components controlling flowering and is regulated by light sensors and an autonomous internal timekeeper called the circadian clock (Sanchez and Kay, 2016; Shim et al., 2017). The central gene of the photoperiod pathway is *CONSTANS* (*CO*), which acts as an integrator of day length

signals and is an output of the clock (Putterill et al., 1995; Suárez-López et al., 2001; Valverde, 2011).

CO encodes a protein with two conserved protein domains: two B boxes located at the amino terminus, involved in protein-protein interactions, and a carboxyl CCT (CONSTANS, CO LIKE, TIMING OF CAB1) domain, which includes a nuclear transport signal and mediates interactions with DNA and diverse proteins (Laubinger et al., 2006; Valverde, 2011). Recently, a role for the central part of CO in regulating floral senescence has been proposed (Serrano-Bueno et al., 2022). CO is a hub in the photoperiodic regulatory network; it receives signals from a multitude of different pathways, such as day length and circadian clock (Serrano-Bueno et al., 2021), and triggers the expression of the florigen *FLOWERING LOCUS T* (*FT*), which induces flower differentiation (An et al., 2004). The circadian clock is an endogenous transcriptional clock that produces biological rhythms with periods of 24 h. This inner clock allows plants to synchronize and anticipate external changes and is one of the most important factors regulating flowering. In *Arabidopsis*, the circadian clock consists of three transcriptional loops, the core loop (CCA1, LHY, and TOC1), the morning loop (PRR5, PRR7, and PRR9), and the evening loop (LUX, ELF3, ELF4, and GIGANTEA) (McClung, 2006; Sanchez and Kay, 2016). CO expression and its protein stability are highly regulated by the circadian clock and light inputs (Suárez-López et al., 2001; Valverde et al., 2004; Mizoguchi et al., 2005). The GIGANTEA (GI) and FLAVIN-BINDING, KELCH REPEAT, F-BOX 1 (FKF1) complex participates in this control by regulating CO transcription by binding to its promoter in the late afternoon and promoting the degradation of CYCLING DOF FACTORS (CDFs), which act as repressors of CO expression (Imaizumi et al., 2005; Sawa et al., 2007). Later, FLOWERING BASIC HELIX-LOOP-HELIX (bHLH) proteins (FBHs) can bind to these genomic sites in the CO promoter to activate its expression (Ito et al., 2012). In addition, The PSEUDO RESPONSE REGULATORS PRR9, PRR7, and PRR5 indirectly promote photoperiodic flowering by repressing *CDF1* (Nakamichi et al., 2007).

Although the CO is highly expressed from late afternoon to dawn, in terms of protein stability, CO is unstable in the dark and stable during the daytime via a process mediated by different photoreceptors and E3 ubiquitin ligases (Valverde et al., 2004). During the daytime, the RING finger-containing E3 ubiquitin ligase HIGH EXPRESSION OF OSMOTICALLY RESPONSIVE GENES1 (HOS1) interacts with CO and targets it for degradation (Lazaro et al., 2012), thus allowing activation of *FT* at the right moment of the day. During the nighttime, COP1 and SPA1 promote CO degradation (Laubinger et al., 2006; Jang et al., 2008). After dawn, several photoreceptors begin to stabilize CO to promote its accumulation during the first hours of the day. In response to blue light, CRY1 and CRY2 interact with COP1 and SPA1 to avoid the degradation of CO by the COP1–SPA1 complex (Yanovsky and Kay, 2002; Liu et al., 2008, 2011; Zuo et al., 2011). Moreover, during the day, two phytochromes affect CO stability in different ways; in response to red light, PHYB interacts with HOS1 to promote the degradation of CO, but, in the late afternoon, PHYA can disrupt the COP1–SPA1 complex to stabilize CO in presence of far-red light (Valverde et al., 2004; Lazaro et al., 2012, 2015; Endo et al., 2013; Hajdu et al., 2015; Sheerin et al., 2015).

In addition to the described photoreceptor pathways, there are some circadian-related proteins that regulate CO accumulation in response to blue light. In the morning, ZEITLUPE (ZTL) forms a complex with GI to inhibit CO stability (Song et al., 2014), but, in the afternoon, blue light enhances CO accumulation by interacting with FKF1 (Song et al., 2012). In fact, FKF1, GI, and CO could form a complex that stabilizes CO (Song et al., 2014). Recently, it has been described that PRRs stabilize CO and promote flowering in response to day length (Hayama et al., 2017). CO stability and its role as transcriptional regulator are both affected. DELLA proteins, the immunophilin FKBP12, the RING domain protein BOI, the B-box zinc-finger 19 (BBX19) and miP1a, and the chromatin remodeling factor PICKLE (PKL) can regulate CO transcriptional function in different ways (Wang et al., 2014, 2016; Nguyen et al., 2015; Graeff et al., 2016; Xu et al., 2016; Jing et al., 2019; Serrano-Bueno et al., 2020). Therefore, CO function is tightly regulated by multiple pathways, all of them ensuring the precise activation of *FT* and the initiation of flowering. Regarding other biological processes regulated by CO, it has been described that CO can modify starch metabolism through the activation of the *GRANULE BOUND STARCH SYNTHASE* (*GBSS*) gene (Ortiz-Marchena et al., 2014). CO may also be involved in stomatal opening (Ando et al., 2013) and play a role in floral senescence (Serrano-Bueno et al., 2022). However, the involvement of CO in other physiological processes is still largely unknown.

It has been proposed that two CO-like (COL) proteins may play a role in the regulation of the circadian clock (Ledger et al., 2001). Although CO is traditionally considered an output of the circadian machinery, its potential impact on the circadian clock remains unclear. Indeed, Ledger et al. (2001) observed no significant difference in the free-running periodic leaf movement of 35S:CO (*Ler*) plants after entraining them in neutral day conditions (12:12). However, since CO presents a CCT domain in its carboxyl terminus, similar to that present in PRRs, that may allow binding to circadian genes promoters (Nakamichi et al., 2010), it was suggested that CO could participate in circadian clock control (Strayer et al., 2000). Circadian network retrograde signaling is often found, and, in this study, we provide conclusive evidence that, in addition to being an output of the clock, CO can also regulate the expression of key genes involved in the circadian time pacer. Therefore, the transcriptional programs controlling the floral transition and the circadian clock are intertwined, constituting a complex system exhibiting feedback loops. Omics techniques based on high-throughput sequencing have recently been applied to unravel this system. However, these data are commonly fragmented, and molecular systems biology approaches are necessary to integrate them and obtain a global comprehension of the interactions between the transcriptional programs controlling the floral transition and the circadian clock.

Network theory constitutes one of the central paradigms in data integration and analysis in molecular systems biology (Barabási, 2015). The integration of massive amounts of omics data has helped generate biological networks for photosynthetic organisms that reveal emergent properties and improve the understanding of processes such as the evolution of CO-like transcription factors (TFs) in Viridiplantae (Romero-Campero et al., 2013), the conservation of circadian patterns across the plant phylogenetic tree (de los Reyes et al., 2017), carbon

mobilization during the floral transition in *Arabidopsis* (Ortiz-Marchena et al., 2014), and the involvement of hormonal control (Serrano-Bueno et al., 2022). In this work, we have constructed a transcriptional gene network by integrating deep sequencing of chromatin immunoprecipitation (ChIP) data generated from key TFs involved in the floral development/transition and circadian clock control. Including data on CO into the analysis of this network allowed us to propose a new function for photoperiodic signaling: the formation of a feedback loop regulating the circadian clock in *Arabidopsis*.

RESULTS

Transcriptional networks reveal a connection between the circadian clock and photoperiodic signaling

In order to examine the interplay between the transcriptional programs controlling the circadian clock and photoperiod, we analyzed ChIP sequencing (ChIP-seq) data from 33 *Arabidopsis* TFs involved in light signaling, flowering, and the circadian clock and built a transcriptional network called CircadianFloralNet (Figure 1A, Supplemental Figure 1A and 1B). This network is composed of 20 601 nodes and 89 377 edges, comprising 75% of the *Arabidopsis* genome (Supplemental Figure 1A). We also generated from CircadianFloralNet a transcriptional gene network containing only the analyzed TFs and their interactions. This network constitutes the regulator core of CircadianFloralNet and was called CircadianFloralTFNet (Supplemental Figure 1B). Therefore, CircadianFloralTFNet is a transcriptional gene network that captures the transcriptional program governing the interaction between the circadian clock, light, and the flowering process. CircadianFloralNet is a scale-free network showing a power-law node-degree distribution (Supplemental Figure 1C) according to the Kolmogorov–Smirnov test (Goldstein et al., 2004). Furthermore, it is a small-world network, implying that the distance between two random nodes is shorter than expected (Supplemental Figure 1D). These topological properties indicate that transcriptional programs governing these processes are highly connected (Wagner and Fell., 2001; Tong et al., 2004; Yook et al., 2004).

The potential input of photoperiod in this network was determined by carrying out a genome-wide analysis of ChIP-seq experiments in 35S:CO and *co-10* 7-DAG (days after germination) seedlings around Zeitgeber time (ZT) 14 under long-day conditions (LD) using specific CO antibodies (Serrano-Bueno et al., 2020). The analysis of CO ChIP-seq data identified 3214 peaks and 2418 putative target genes (Supplemental Table 1), and we included this information into CircadianFloralNet. Next, we generated CircadianFloralTFNet including CO and classified the nodes into light, flowering, or clock genes based on their TAIR (The Arabidopsis Information Resource) classifications (Figure 1A). CO was found to bind to the promoters of the *PHYTOCRHOME INTERACTING FACTOR 1* (*PIF1*), *PIF3*, and *PIF4* genes related to light signals and to the promoters of *SOC1* and *SVP*, which are specifically associated with flowering time control. However, all genes clustering in the clock function in CircadianFloralTFNet, including *CCA1*, *LHY*, *TOC1*, *PRR5*, *PRR7*, and *PRR9*, showed one or several peaks of CO binding on their promoters (Figure 1A), indicating that CO bound to the promoters of genes involved in circadian rhythm regulation, including the core components of the clock, *CCA1/LHY* and *TOC1*.

A network motif analysis on CircadianFloralTFNet was performed to identify relevant non-random components in the interactions between the circadian clock and photoperiod. Network motifs are subgraphs that appear in an observed network significantly more frequently than they do in other comparable networks (Milo et al., 2002; Shen-Orr et al., 2002; Stone et al., 2019). Therefore, we tested the significance of all possible subgraphs consisting of one, two, or three nodes by generating 100 000 random graphs with the same topological features as the original network. The most represented motifs identified are shown in Supplemental Figure 1E. One of the most significant and common motifs was the “feedback loop with output” ($p < 10^{-5}$), which meant that there is a high interconnection among the transcriptional programs analyzed.

The connectivity we identified in CircadianFloralNet confirmed the results of previous studies (Suárez-López et al., 2001; Imaizumi et al., 2005; Sawa et al., 2007) that established that CO expression was regulated by the circadian clock. Specifically, *PRR5* binds to *cis* elements in the *CO* promoter in order to regulate its expression, and, consequently, both genes are connected in CircadianFloralNet (Figure 1A). Additionally, a substantial number of genes of the *CO*-like (*COL*) family are regulated by *PRR5* and other central proteins of the circadian clock, such as *CCA1* and *PRR7*, as shown in the subnetwork presented in Supplemental Figure 1F. Since the feedback loop is a network motif in CircadianFloralTFNet and *PRR5* regulates *CO*, it was expected that *CO*, in turn, would also regulate the expression of *PRR5*. We verified *CO* binding to the *PRR5* promoter through ChIP-seq and ChIP-qPCR experiments (Supplemental Figures 1G and 4B). This result implies that one of the interactions between the flowering program and the circadian clock is exerted by *CO* and *PRR5*.

In fact, based on ChIP-seq data, *CO* and *PRR5* constitute a “feedback loop with multiple output” motif, represented in Figure 1B, that may regulate a set of common target genes related with the circadian clock (*CCA1*, *LHY*, *RVE1,8*, *TOC1*, *PRR7,9*, and *LNK1,2*) and photoperiod signaling (*GI*, *CDFs*, *BBXs*, *GBBS1*, and *BAM1,9*).

CONSTANS alters the expression of circadian clock genes

RNA sequencing (RNA-seq) experiments from different plants, including general expression (35S:CO), phloem specific, where *CO* floral function takes place (*SUC2:CO*), and *Col-0* (wild type [WT]), were carried out to investigate the proposed effect of *CO* on the clock (GSE236178). We extracted RNA from LD (16 h light:8 h night) grown seedlings collected in the evening at ZT14, where *CO* activity is at a peak (Valverde et al., 2004). Similarly, we included an available RNA-seq dataset of *Col-0* and *co-10* mutant plants grown in continuous light (LL) (Gnesutta et al., 2017; GSE205675). After analyzing the data via standard pipelines (see section “methods”), we found 637 and 1765 upregulated genes in 35S:CO and *SUC2:CO* compared to WT, respectively, and 714 downregulated genes in *co-10* plants (Supplemental Table 2). To obtain high-fidelity *CO*-regulated genes, we overlapped the three sets of genes in a Venn diagram consisting of 70 intersecting genes (Figure 1C, Supplemental Table 3). According to the GO-term enrichment analysis, these genes are involved in several biological processes, such as the

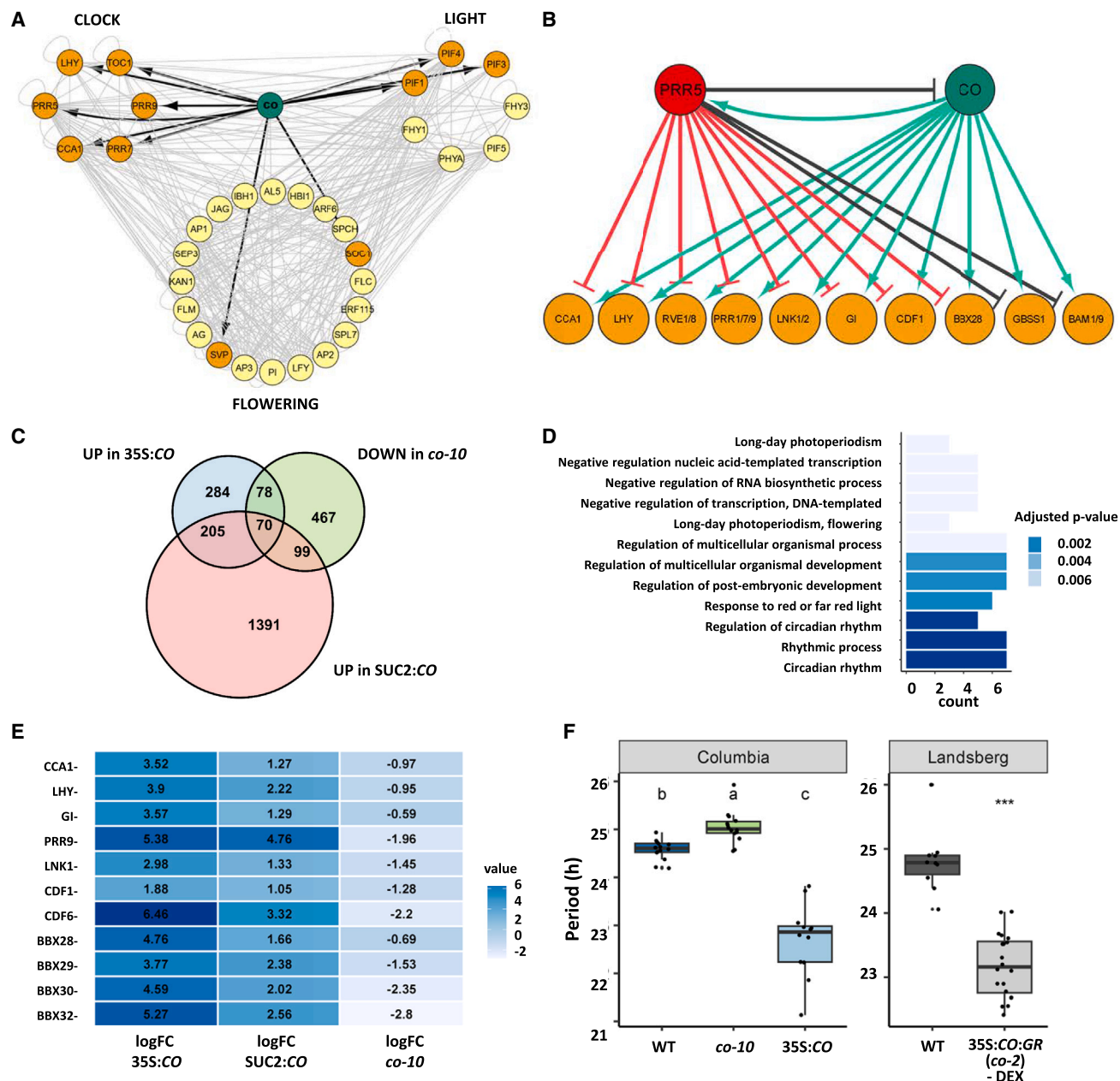


Figure 1. CONSTANS alters the circadian clock system in *Arabidopsis*.

(A) Graphical representation of CircadianFloralTFNet, a derived network including only the analyzed TFs and their interactions. Nodes are clustered in CLOCK, LIGHT, or FLOWERING. CO is colored in green, CO target genes in dark orange and non-target genes in yellow.

(B) Feedback loop with multiple outputs containing CO and PRR5 as regulators with a set of common target genes involved in the circadian clock and photoperiodic signaling. PRR5 expression data (Li et al., 2020) and CO expression data (this paper) have been analyzed to color the edges: Green, red, and black edges indicate activation, repression, and DNA binding, respectively.

(C) Venn diagram representing downregulated genes in the *co-10* mutant (green), upregulated genes in SUC2:CO (pink), and upregulated genes in 35S:CO plants (blue). The intersecting 70 genes (SuperExactTest, $p = 1.12 \times 10e-114$) are considered high-fidelity CO-regulated genes.

(D) GO-term enrichment analysis over the intersection between downregulated genes in *co-10* mutants and upregulated genes in CO-overexpressing lines, indicating that they are significantly involved in circadian rhythm processes.

(E) Table heatmap showing the change of expression (log fold change) between *co-10*, 35S:CO, SUC2:CO, and the control (WT) for circadian-related genes.

(F) Left: period distribution of rhythmic leaf movement in Columbia ecotype Col-0 (WT), *co-10*, and 35S:CO. Right: period distribution of rhythmic leaf movement in Landsberg ecotype, WT (*Ler*), and 35S:CO:GR (*co-2*) without (–) added dexamethasone (DEX). Plants were grown in LD until 7 DAG, transferred to LL, and monitored for six more days. * $p < 0.05$; *** $p < 0.001$, one-way ANOVA and Tukey's honestly significant difference (HSD).

response to light stimuli or photoperiodism and, as we expected, rhythmic processes and circadian rhythm with the highest probability (Figure 1D, Supplemental Table 4). Specifically, several key circadian clock genes (*CCA1*, *LHY*, *GI*, *PRR9*, and *LNK1*) and clock-output genes (*CDF1*, *CDF6*, *BBX28*, *BBX29*, *BBX30*, and *BBX32*) showed higher expression in *SUC2:CO* and *35S:CO* plants and lower expression in *co-10* mutants (Figure 1E, Supplemental Figure 2).

Further assessments were made to test if CO was able to modify the diurnal pattern of expression of other genes. RNA-seq data from a transcriptome of Col-0 plants under LD conditions in a 24-h period (GSE43865, Rugnone et al., 2013) were analyzed and estimated gene expression levels at ZT2, ZT6, ZT10, ZT14, ZT18, and ZT22 quantified. Using this analysis, we identified genes exhibiting a diurnal pattern of expression and classified them into clusters depending on the time point at which they reached their minimal and maximal expression (see section “methods”). To identify the specific diurnal patterns affected by CO, we studied the statistical significance of the intersections between the daily gene clusters and the activated genes in *35S:CO* at ZT14. Only three diurnal clusters presented a significant intersection according to Fisher’s exact test, as shown in Supplemental Table 5 ($p = 4.72e-66$, $1.21e-08$, $5.02e-42$, and $6.31e-12$). All the clusters showing a significant intersection presented a morning peak and an evening/afternoon trough. We concatenated these clusters into a single group called the “morning-phased” cluster and, again, the intersection of these genes with the activated genes in *35S:CO* was significant (Fisher’s exact test, $p < 2.2e-16$) (Supplemental Figure 3A), in agreement with previous studies (Gnesutta et al., 2017). This result shows that CO activates the expression of genes in the evening that naturally exhibit their minimum expression at that time of day, thus altering their daily patterns.

In order to confirm the effect of CO on the clock, using RT-qPCR, we measured the expression of some of the genes regulated by CO every 4 h during a 24-h period in WT, *co-10* mutant, and *35S:CO* plants (Supplemental Figure 3B). We found that *PRR5*, *PRR7*, *GI*, and clock-output genes such as *BAM9* were activated in *35S:CO*, especially at ZT14, when CO protein is stabilized under LD (Suárez-López et al., 2001) and down in *co-10* in *PRR5* and *BAM9*. This reflected the fact that CO overexpression, and its absence, altered the daily expression of some clock genes.

Further assessments were made to test if CO was able to alter physiological aspects of the circadian behavior of *Arabidopsis*. In plants, one of the most well-known and characterized circadian clock outputs is the daily rhythmic movement of leaves that has been used to identify several key components of the circadian clock (Wang and Tobin, 1998). We tracked this movement in LD-entrained 7-DAG seedlings from WT, *co-10*, and *35S:CO* plants transferred to LL and estimated the period of the leaf movement for 6 days. As shown in Figure 1F, *co-10* mutant showed a longer period than WT, and *35S:CO* plants exhibited a significant shorter period, similar to *prr5-1* mutant (ANOVA; $p = 0.0312$ and $1.04e-11$, respectively) (Supplemental Figure 8B). Furthermore, we investigated the impact of CO on the rhythmic leaf movement in the Landsberg *erecta* (*Ler*) ecotype using the dexamethasone (DEX)-inducible line *35S:CO:GR* in *co-2* mutant background. Surprisingly, the *35S:CO:GR co-2* (-DEX) plants ex-

hibited a significantly shorter period compared to WT plants (Figure 1F, right), contrasting with the observed effect in *co-10* line (Student’s *t*-test; $p = 6.521e-08$). In addition, we performed an independent experiment applying dexamethasone to *35S:CO:GR (co-2)* plants. We verified that, after inducing the expression of CO, the short-period phenotype is compensated, reaching WT levels (Supplemental Figure 8A). As *Ler* shows a distinct flowering behavior to Col-0, the effect of CO on the Landsberg circadian system can be an interesting future research subject. Altogether, the change in nastic rhythms shown in *co* mutants is a strong evidence that CO is involved in circadian clock modification.

ChIP-seq data from *35S:CO* and *co-10* plants at DAG7 was further analyzed to determine if CO could be altering the circadian rhythms by direct binding to clock gene promoters. The CO ChIP peak distribution was found to be enriched mainly in promoter regions near the transcription start sites (65%), and, to a lesser degree, regions up to 2 kb away (10%), downstream regions (6%), and distant intergenic regions (7%), indicating that it is probably a *bona fide* TF (Figure 2A). Next, we compared the ChIP-seq data with the upregulated genes in *35S:CO* and *SUC2:CO* (Supplemental Figure 4A), obtaining a significant overlapping (SuperExactTest; $p = 5.706e-209$). We found that almost 23% (550 out of 2418) of the CO target genes were also affected in both overexpressor lines, including its main target, the floral integrator *FT*, as well as other photoperiodic growth/development related genes, such as *CDF3* and *CDF6*, and key circadian clock genes, such as *PRR5*, *LHY*, *GI*, *RVE8*, and *RVE4* (Supplemental Figure 4B). Binding of CO to clock gene promoters suggested that CO was able to alter not only photoperiodic genes expression, as previously suggested (Onouchi et al., 2000), but also the expression of circadian clock-related genes.

CO regulates *FT* expression by binding to its promoter in association with NF-Y/HAP heterodimers to bind to CCAAT elements (Wenkel et al., 2006) and to CO-responsive element (CORE) sites (Tiwari et al., 2010). However, recently, it was shown that CO imparts DNA sequence specificity to the NF-Y heterodimer resembling a histone pocket, thus allowing the complex to bind to the CCACA element (Gnesutta et al., 2017; Shen et al., 2020). This CCACA element exhibits significant similarity to the morning element, for which the AACCAC motif has been described as an essential element for its function (Harmer and Kay, 2005; Michael et al., 2008). We performed unbiased DNA motif discovery analysis in the CO ChIP-seq data and confirmed the presence of a motif containing the CCACA element ($p > 10^{-19}$) and another motif resembling a CORE-like element ($p > 10^{-13}$) (Figure 2B); unexpectedly, we identified a G box (CACGTG) that was significantly enriched ($p > 10^{-18}$) in CO-binding peaks. Our analysis showed that CO could bind to G-box sites in *CCA1*, *LHY*, and other loci (Figure 2C) but not on the *FT* promoter, where it was associated exclusively with CCACA and CORE sites, revealing an NF-Y/HAP-independent mechanism.

Together, these results suggested that CO is not only an output of the circadian clock pathway but also a factor exerting feedback regulation over key circadian clock genes and circadian patterns, implying a novel function for CO in altering rhythmic processes in *Arabidopsis*.

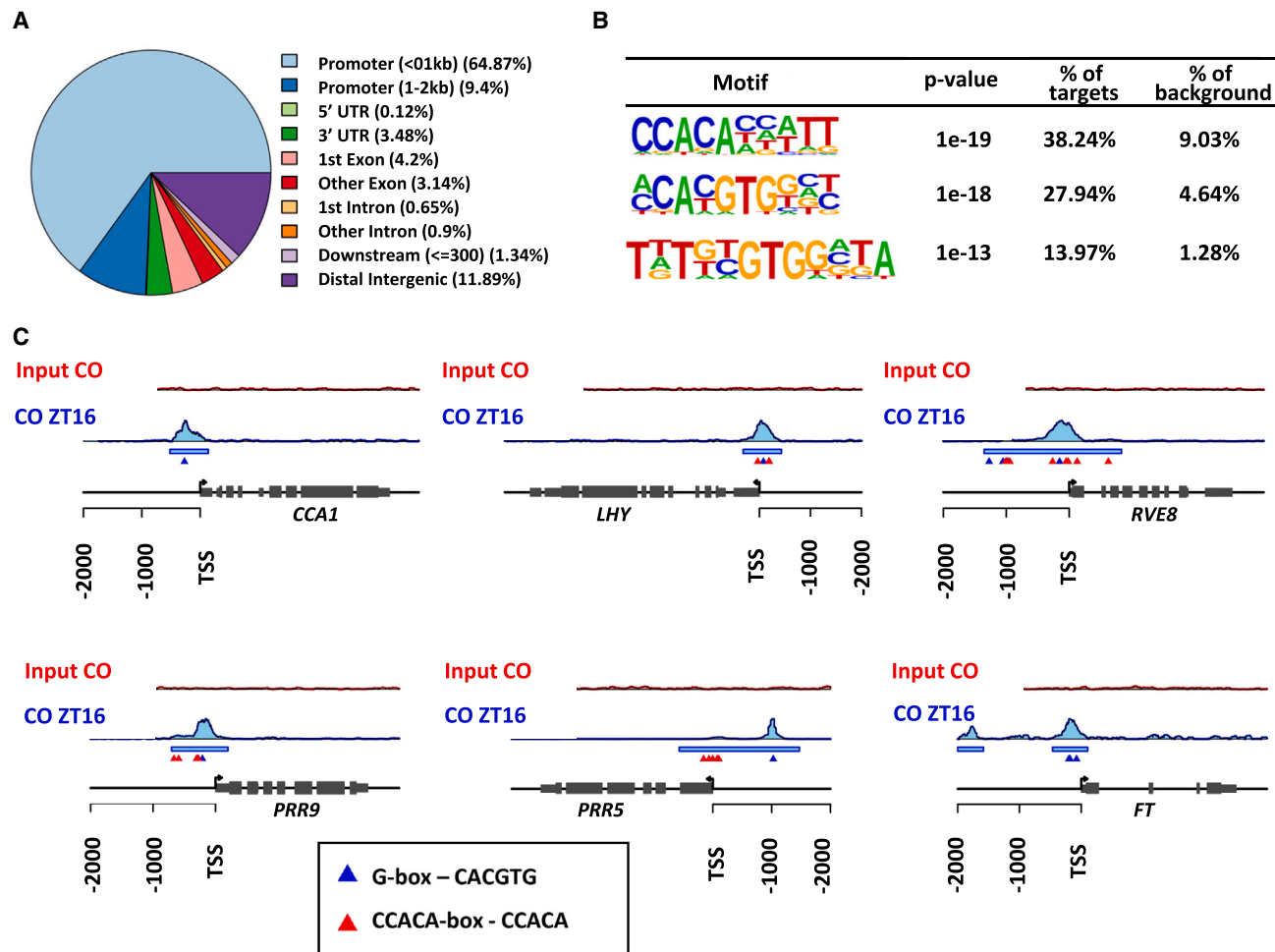


Figure 2. CO binds to clock gene promoters.

(A) Pie graph representing the genome-wide distribution of CO peaks. Most of the binding sites (64.87%) are located in promoters (≤ 1 kb).

(B) *De novo* DNA motif identification over the CO-binding sites using HOMER software and the % of distribution in CO peaks.

(C) ChIP-seq visualizer views of CO occupancy of circadian-related genes. The binding profile of immunoprecipitation and input experiments are colored red and blue, respectively. Peaks detected by MACS2 are indicated by blue rectangles. CCACA (red triangles) and G-box elements (blue triangles) located at peaks are also showed.

CO, PRRs, and HY5 share genomic-binding sites in some circadian clock-regulated genes

G-box motifs are the binding sites of bZIP and bHLH TFs and have been described in the transcriptional regulation exerted by PRRs, thus suggesting an association with these TFs (Liu et al., 2016). Under short days (SD, 8 h light, 16 h dark), with a long dark period, the night-inducible bHLH PIFs have been described to bridge the binding of PRRs to DNA to sequentially repress shared target genes related to growth, such as *CDF5* (Martin et al., 2018). Additionally, PIF4 is involved in the temperature-dependent activation of *FT* through binding to CO under SD (Fernández et al., 2016), but, as PIFs are unstable in the light, no involvement on the clock under LD was reported. On the other hand, the bZIP LONG HYPOCOTYL 5 (HY5) is a light-inducible TF (Osterlund et al., 2000) that binds to G boxes (Lee et al., 2007; Young et al., 2008; Zhang et al., 2011; Binkert et al., 2014), and *hy5* mutations affect flowering (Bhagat et al., 2021) and the clock (Hajdu et al., 2018). It has also been described that HY5 can interact with BBX family proteins from

group IV (BBX21–25) through the b-box domain to activate or inhibit its role in photomorphogenesis (Datta et al., 2007; Job et al., 2018; Bursch et al., 2020). Therefore, HY5 was a good candidate to act as bridge mediating the binding of PRR5 and CO to clock-related gene promoters during the day under LDs. HY5 is also degraded by the COP1/SPA1 complex during the night (Osterlund et al., 2000), similar to CO (Jang et al., 2008), and it has been shown that CO and HY5 interact with the diurnal chromatin remodeling factor PKL (Jing et al., 2013, 2019).

Indeed, when we compared the genome-wide analysis results for the ChIP-seq data for PRR5 (Nakamichi et al., 2012) and ChIP-on-chip data for HY5 (Lee et al., 2007) with the ChIP-seq data for CO, a significant overlap between the direct targets of PRR5, HY5, and CO was found (SuperExactTest; $p < 2.62e-14$) (Figure 3A). After carrying out a DNA motif discovery analysis over the promoter sequences (1 kb) of the different gene sets of the Venn diagram (Figure 3A right, Supplemental Table 6), we found a motif resembling the CCACA element (Gnesutta et al., 2017) in the

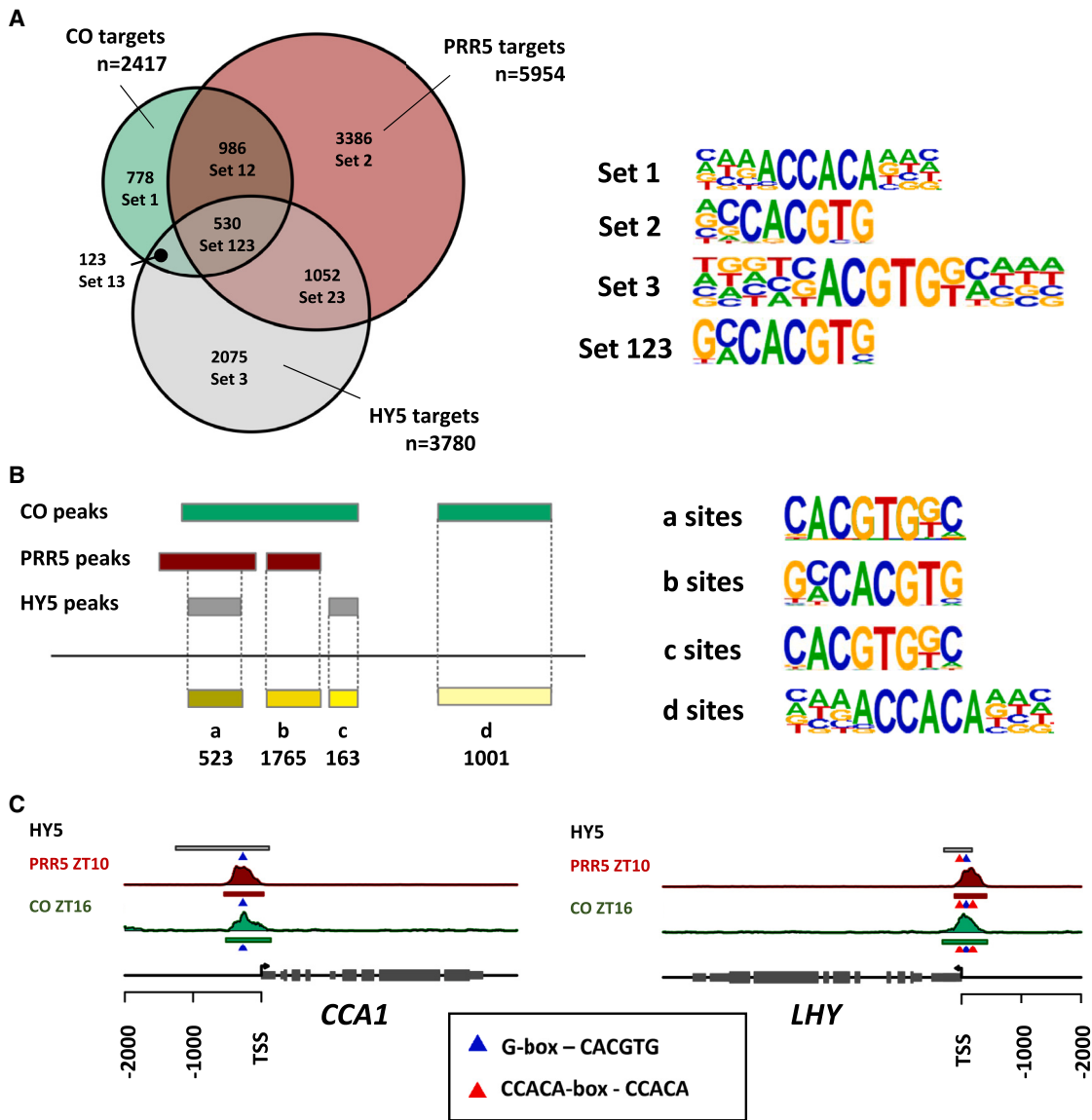


Figure 3. HY5, PRR5, and CO genome-binding analysis.

(A) Left: Venn diagram showing the significant intersection (SuperExactTest, $p < -10^6$) of CO (green), HY5 (gray), and PRR5 (red) targets. Right: DNA motifs enriched in the promoters of the different gene sets. Sets 1, 2, and 3 represent the exclusive target genes of CO, PRR5, and HY5, respectively. Set 12 comprises the genes targeted by both CO and PRR5, set 13 includes the genes targeted by both CO and HY5, and set 23 contains the genes targeted by both HY5 and PRR5. Finally, set 123 represents the intersection of target genes between CO, HY5, and PRR5.

(B) Left: graphic scheme of the peak intersection analysis. The “a” sites correspond to the intersection of the CO, HY5, and PRR5-binding peaks. The “b” sites represent the overlap between the CO and PRR5 peaks, while the “c” sites indicate the intersection between the CO and HY5 peaks. Finally, the “d” sites are regions exclusively bound by CO. Right: DNA motif enrichment analysis performed in each retrieved peak set.

(C) Peak visualizer views of HY5 (gray), PRR5 (red), and CO (green) binding to *CCA1* and *LHY* promoters. G-box and CCACA elements are indicated by blue and red triangles, respectively.

gene promoters regulated exclusively by CO (set 1), indicating that it binds to these regions via an NF-CO trimer. A matrix containing a G-box motif was enriched in the genes regulated by PRR5 (set 2), as described in previous studies (Liu et al., 2016). Notice that the most significant enriched DNA matrices come from bHLH TF ChIP-seq studies (Supplemental Table 6), suggesting that PRR5 regulates the transcription of these genes in association with bHLHs (Martín et al., 2018). However, a DNA matrix containing an E-box motif ACGTG was recovered from the genes regulated by HY5 (set 3). This suggests a certain degree of specificity im-

parted by the protein with which HY5 associates. We also found a G-box motif enriched in the gene promoters bound by CO, HY5, and PRR5 (set 123), indicating that this DNA element plays a key role in the transcription of these clock-regulated genes. Furthermore, the most significant DNA matrices were described in bZIP TF ChIP-seq studies (Supplemental Table 6).

Next, to support our hypothesis, we followed a similar approach to analyze the genome-wide binding sites of CO, HY5, and PRR5 (Huang et al., 2012; Nakamichi et al., 2012; Liu et al., 2013a, 2016)

(Supplemental Table 7). First, we found a significant overlap between the three sets of binding regions according to permutation tests (adjusted $p < 0.0001$) (Supplemental Table 8). Then, using the *intersectBed* function from *bedtools*, we retrieved the overlapping peaks for the three TFs (a), the intersection between CO and PRR5 sites (b), the intersection between HY5 and PRR5 sites (c), and the genome regions bound by CO (d) (Figure 3B, left). In order to determine the DNA elements involved in the regulation exerted by these TFs, we performed DNA motif discovery analyses over the different binding site sets (Figure 3B, right). A CCACA element was enriched exclusively in the CO-binding sites (d), which is consistent with previous studies based on transcriptomic data (Gnesutta et al., 2017). However, G boxes were enriched in the other intersections, a–c sites (Figure 3B, right). Furthermore, we analyzed ChIP-seq data for other PRR family members at different time points. We found an overlap between the binding sites of CO, HY5, TOC1, PRR5, PRR7, and PRR9 in G-box-containing sites located in clock promoters (Supplemental Figure 5A). All these results indicate that CO and PRR5 bind to a G box to control the transcription of clock-regulated genes, probably in association with a bZIP TF, such as HY5, as shown in Figure 3C for the *CCA1* and *LHY* promoters.

ChIP experiments using GFP-Trap antibodies in 35S:*GFP:HY5* (*hy5-211*) plants were performed to further demonstrate HY5 binding to these sites. We observed an enrichment of these amplicons compared with the control (WT plants) that was absent in the *FT* promoter (Supplemental Figure 5B). These results indicated that HY5 binds to the same sites as CO in these circadian clock promoters but not the CORE site associated with CO in the promoter of *FT*, highlighting that CO has a different function related to circadian rhythm that is largely independent of the photoperiodic flowering pathway.

A cross between *hy5-2* mutant and 35S:CO plants obtaining the double 35S:CO *hy5-2* mutant was performed to confirm the role of HY5 in CO-dependent clock gene transcriptional modification (Figure 4A). These plants showed a small delay in flowering time compared to 35S:CO plants (Figure 4B). 35S:CO *hy5-2* plants showed high expression of CO and no expression of *HY5* mRNA or protein, as confirmed by RT-qPCR (Supplemental Figure 6A) and western blot experiments (Supplemental Figure 6B), respectively. Consequently, the expression of the clock-related genes *CCA1*, *PRR5*, *PRR7*, and *GI* activated by CO was reduced, with values close to WT (Figure 4C, Supplemental Figure 6C), further confirming the role of HY5 in CO-dependent clock gene expression.

ChIP experiments using α CO in the lines 35S:CO, 35S:CO *hy5-2* and *co-10* as control were performed to analyze the contribution of HY5 to the binding of CO to G-box elements. We measured by RT-qPCR the enrichment on the *FT*, *GI*, and *PRR5*-binding sites (Figure 4D). Despite containing equal levels of CO (Supplemental Figure 6B), we observed a reduced enrichment in 35S:CO *hy5-2* at the G-box sites of *PRR5* and *GI*. Contrary to our initial hypothesis, we also observed a reduction in 35S:CO *hy5-2* on the CORE site of *FT*, indicating that HY5 also contributes to CO binding at this locus or that the absence of HY5 changes the conformation of the *FT* promoter, due to the presence of non-canonic E-box sequences (Liu et al., 2013b).

CO, PRR5, and HY5 proteins interact in planta

The interaction between CO and some members of the PRR family was previously shown; this binding stabilizes CO and enhances photoperiodic flowering under LD conditions (Hayama et al., 2017). However, considering that CO and PRR5 bind to the same sites in some promoters and that these two proteins seem to have the opposite effect over transcription, it is possible that CO can gradually remove PRR5 from the DNA and promote transcription, together with HY5. Therefore, a transient complex consisting of HY5, PRR5, and CO during the evening could exist to alter gene expression. To examine this possible ternary complex, we performed different protein-protein interaction approaches.

First, we performed a bimolecular complementation (BiFC) assay in *Nicotiana* between CO, HY5, and PRR5 in pairs, and we observed the interactions between them in the nucleus and found different distribution patterns (Figure 5A, Supplemental Figure 7A). We also performed yeast-two-hybrid (Y2H) experiments with the three main domains of CO (B boxes, middle domain, and CCT domain) to confirm the interaction with both HY5 and PRR5. As can be seen in Figure 5B, and different from the previous results on the binding of other BBXs to HY5 through the B boxes (Bursch et al., 2020), CO interacts with HY5 and PRR5 through the middle domain and, to a lesser extent, the CCT domain. To further investigate if there could be a ternary complex, we tested the colocalization of the three proteins in the nucleus of *Nicotiana* cells. To do this, we reconstituted the YFP fused to HY5 and PRR5 and co-infiltrated a CO:CFP construct. We detected a significantly higher colocalization in speckles, compared with the control with CFP alone (Student's *t*-test; $p = 4.989e-04$) (Figure 5C). Following this approach, we measured fluorescent resonance energy transfer (FRET) between CFP and YFP through a sensitized emission method, and we found higher values in the CO/HY5/PRR5 combination than in the negative controls, confirming the close interaction among the three proteins (Figure 5D, Supplemental Figure 7B).

Since CO and HY5 physically interact and both proteins bind to the same regions in clock gene promoters, we investigated if they could associate with DNA when combined. To examine this possibility, the immunoprecipitated complex resulting from the ChIP experiment was analyzed by immunoblot using anti-HY5 antibodies. We detected HY5 protein in the 35S:CO sample but not in the control (Figure 5E), confirming the presence of a complex between CO-HY5 and DNA.

The clock-related leaf movement was also affected in *prr5-1* and *hy5-2* mutants, showing an acceleration of the period compared to WT plants (Supplemental Figure 8B).

Together, these results indicated that these three proteins could form a complex that binds to the DNA, acting HY5 as scaffold, since this type of TF, bZIP, is largely described to be capable of directly binding to DNA (Chattopadhyay et al., 1998; Abbas et al., 2014; Binkert et al., 2014).

DISCUSSION

A network science perspective is essential for understanding complex interconnected systems (Barabási, 2015). Transcriptional

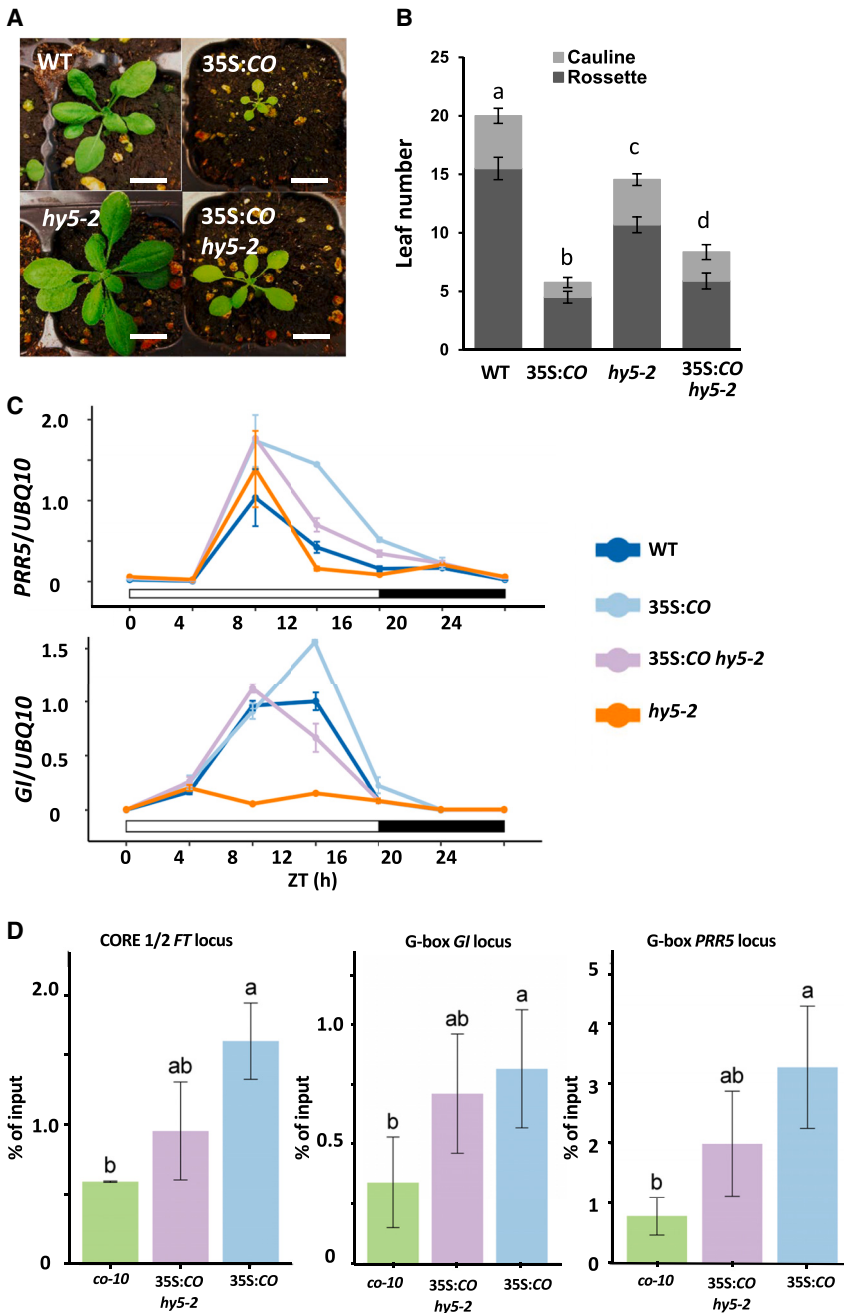


Figure 4. Genetic interaction between CO and HY5.

(A) Pictures of WT (Col-0), 35S:CO, *hy5-2*, and 35S:CO *hy5-2* plants at DAG15.

(B) Flowering time of WT, 35S:CO, *hy5-2*, and 35S:CO *hy5-2* plants measured as total leaf number.

(C) The 24-h expression of CO target genes *PRR5* (above) and *Gl* (below) in WT, 35S:CO, *hy5-2*, and 35S:CO *hy5-2* plants at ZT14, DAG 15.

(D) ChIP-qPCR of amplicons located in the *FT* (CORE 1,2 sites), *Gl* (G-box site), and *PRR5* (G-box site) promoters in *co-10* (green), 35S:CO *hy5-2* (magenta), and 35S:CO (blue) plants using α CO. Transcription start site region of *ACT2* gene was used as control for normalization. Error bars indicate the SD from three independent experiments. $p < 0.05$, one-way ANOVA and Tukey's HSD.

programs governing circadian clock and photoperiodic pathways showed a high relatedness in CircadianFloralNet according to its scale-free and small-world properties, which revealed many unexplored connections (Figure 1, Supplemental Figure 1). Much debate has focused on the validity of analyzing gene network motifs because they are components of large and complex networks (Mellis and Raj, 2015). Indeed, CircadianFloralNet represents all potential interactions under many conditions, tissues, growth stages, and times of day; furthermore, smaller and insulated networks have to be considered. Thus, the network motif formed by *CO* and *PRR5* functions in the evening under LD conditions (Figure 1B).

In recent years, the circadian clock in *Arabidopsis* has emerged as a complex regulatory system; it is not a simple

molecular timer but a regulator of multiple processes involving hormone, metabolism, and stress pathways, some of which exert feedback regulation on the clock (Sanchez and Kay, 2016). Indeed, several TFs that contribute to clock function have been identified (McClung, 2014) and it has been proposed that different tissues may show differences in the clock (Endo et al., 2014; Qin et al., 2023). *CO* function is strongly regulated at both the transcriptional and post-translational levels in *Arabidopsis*, indicating that the photoperiodic pathway has been subjected to high selective pressure (Romero and Valverde, 2009). Other than flowering transition and reproductive development, no other functions had been described for *CO*, but recent studies suggested that it could regulate floral jasmonate signaling (Serrano-Bueno et al., 2022), seed size (Yu et al., 2023a), and circadian genes (Gnesutta et al., 2017). Here, we show that *CO* alters the circadian clock by binding to the promoters of key clock-related genes (Figure 2C, Supplemental Figure 4B), revealing an undescribed function.

Therefore, there is an even more complex regulation between the circadian clock and photoperiod pathways than previously shown.

Several members of the B-box zinc-finger family have been identified as regulators of the circadian clock. Among them, recent studies have shown that BBX19 (subfamily IV) and BBX28/BBX29 (subfamily V) interact with PRRs to finely regulate the circadian clock in *Arabidopsis* (Yuan et al., 2021; Yu et al., 2023b). BBX19 shows DNA-binding activity and negatively regulates the expression of morning-phased genes by associating with G boxes. However, its binding affinity is reduced in the *prr9-1 prr7-3* and *prr5-1 prr7-3* mutants. BBX28 and BBX29 also magnify the PRR5 repression activity, although there is no evidence demonstrating their

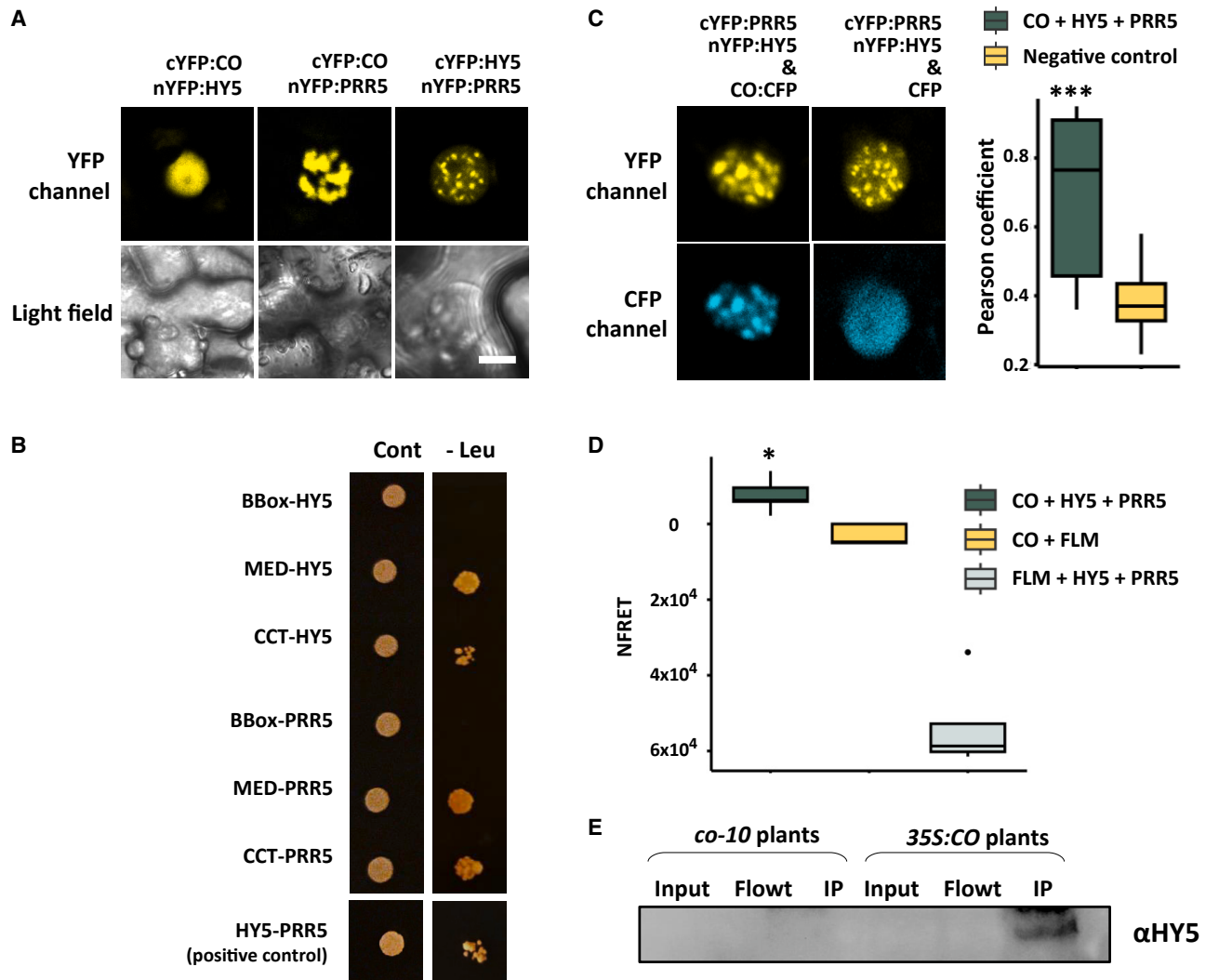


Figure 5. Protein interaction between CO, HY5, and PRR5.

(A) Confocal images of CO, HY5, and PRR5 interactions using BiFC assays in *Nicotiana* leaves.

(B) Y2H assays showing the interaction between different parts of CO (B-box, middle, and CCT domains) with HY5 and PRR5. Panels show 3-day-old colonies grown in control and selective media.

(C) Colocalization experiments of CO, HY5, and PRR5 proteins. YFP was reconstituted by fusing N- and C-terminal parts to HY5 and PRR5; the full-length sequence was fused to CO. The colocalization between both fluorophores was measured by Pearson correlation compared to a negative control.

(D) FRET analysis between CO, HY5, and PRR5. CO was fused to CFP and YFP was reconstituted by nYFP:HY5/cYFP:PRR5. CFP:FLM and YFP:FLM were used as negative controls. The proteins were coexpressed in *N. benthamiana* leaves, and normalized FRET (nFRET) was measured in 10 cells.

(E) Immunodetection of the HY5 protein with αHY5 in chromatin immunoprecipitation experiments (using αCO) of 35S:CO and *co-10* plants.

direct DNA association. Therefore, as they lack the CCT DNA-binding domain, they indirectly lead to alterations in the clock mechanism by forming complex with PRRs and enhancing their repression. In this study we demonstrate that the binding of CO to the G boxes results in the activation of gene expression, in opposition to the PRRs (Figure 1B).

Moreover, more than two decades ago, Ledger et al. (2021) observed a shorter leaf movement period when *COL1*- and *COL2*-overexpressing plants were monitored under free-running conditions after growing the plants in neutral day (12:12). Here, we detect the same behavior in the 35S:CO line entrained in LD conditions (Figure 1F). This suggests a potential

redundancy among CO, *COL1*, and *COL2* in their impact on the circadian clock, which could explain the mild phenotype of the single *co* mutant. Notably, Ledger et al. found no significant differences in the periodic leaf movement between 35S:CO and WT (*Ler*) plants. However, it is crucial to consider that these plants were grown under non-inductive conditions for CO (neutral day), which might explain the disparities with our results. Following the notion that CO serves as a seasonal cue, we propose that these three TFs may function sequentially during the day, similar to the PRR family, with CO being mostly active under LD conditions.

PRRs have been described as repressors of their direct target genes. According to our network based on ChIP-seq data,

PRR5 could bind to the CO promoter. Nevertheless, PRRs cause a global positive effect over the photoperiod pathway and CO-FT module regulation, since they stabilize CO (Hayama et al., 2017) and repress *CDF1* expression, triggering the net activation of CO and FT expression (Nakamichi et al., 2007). Then, the control of PRR5 gene expression by CO establishes a positive feedback loop between the circadian clock and the photoperiodic pathway (Supplemental Figure 1G). In addition to PRRs, CO binds to the *GI* promoter (Supplemental Figures 4B and 5A). Since *GI* exerts an activating role over CO (Imaizumi et al., 2005; Sawa et al., 2007; Song et al., 2014), this could also form a positive feedback loop to enhance and fix the photoperiodic response in the afternoon under LDs. The crosstalk between flowering and the circadian clock exerted by CO could help to explain the existence of tissue-specific clocks (Endo et al., 2014; Qin et al., 2023). These results support the already established concept of complex interlocking loops instead of a unidirectional system composed of input-oscillator-output.

Moreover, it seems that in addition to affecting clock genes such as PRR5 or *GI*, CO could regulate circadian clock target genes, including a significant number of PRR5 targets. This set of genes would be repressed by PRR5 and activated by CO, forming a transcriptional switch (Figure 1B). In order to move from a vegetative phase to a reproductive phase, massive changes in gene expression are needed in plants; thus, CO could provide the activation of a set of repressed genes and promote the phase transition (Figure 6).

There has been a long controversy about whether CO could act as a TF or as a coactivator (Blackman and Michaels, 2010). Recently, it has been discovered that CO can directly bind to CORE elements and associate with NF-Y/HAP heterodimers to bind to CCACA elements, acting as an activator of gene expression (Wenkel et al., 2006; Tiwari et al., 2010; Gnesutta et al., 2017). Indeed, CO activity can be controlled by the formation of different types of protein complexes, even repressor complexes formed by TOPLESS (Graeff et al., 2016). Here, we demonstrate that CO is able to bind to G-box elements in DNA through the bZIP TF HY5, a TF involved in many light processes and pathways (Gangappa and Botto, 2016). Together, these findings show a great plasticity in CO function as a transcriptional regulator and its ability to recruit circadian clock machinery at the end of a long day. Depending on its partners, CO will exhibit different effects over transcription and affinity for different genome-binding sites, thus conferring high plasticity to plants in response to daylength changes.

METHODS

Plant material and growth conditions

Plant lines in the Col-0 background used in this study included 35S:CO (Onouchi et al., 2000), 35S:CO:GR (co-2) (Simon et al., 1996), SUC2:CO (Hayama et al., 2017), *co-10* (SAIL_24_H04), *hy5-2* (SALK_056405C), 35S:GFP:HY5 (*hy5-211*) (kindly provided by Dr Vicente Rubio), and *prr5-1* (SALK_006280; Michael et al., 2003). 35S:CO *hy5-2* double-mutant plants were generated by crossing 35S:CO with *hy5-2* to form homozygotes. *Arabidopsis* seedlings were grown in an SG-1400 phytotron (Radiber SA, Spain) under an LD light regime with temperatures ranging from 22°C (day) to 18°C (night) and 100 $\mu\text{E m}^{-2} \text{s}^{-1}$ light intensity. *Arabidopsis* seeds were stratified for 3 days at 4°C in the dark and later grown in Murashige & Skoog (MS) medium. For gene expression ana-

lyses, *Arabidopsis* seedlings were collected every 4 h during a complete LD. For monitoring leaf movement, seedlings were grown in soil for 7 days under LD conditions, transferred to LL conditions, and examined for 6 or 7 days.

ChIP experiments

ChIP was carried out as described previously (Bowler et al., 2004) with minor modifications to improve binding enrichment (Lau and Bergmann, 2015). Plants were grown for 7 days under LD conditions and 9 g of seedlings were harvested at ZT12-ZT16. Then, plant tissue was cross-linked in a vacuum concentrator in presence of 1 mM DSG for 10 min, 1% (v/v) formaldehyde for 20 min, and finally 0.125 M glycine to stop crosslinking. Later, the tissue was ground in liquid nitrogen and chromatin was isolated. Chromatin complex immunoprecipitation was performed using α CO (Serrano-Bueno et al., 2020) and GFP-Trap agarose beads (ChromoTek) to capture CO and HY5 proteins, respectively. After immunocomplex capture, DNA was eluted from the beads, crosslinked with proteins, reverse transcribed, and isolated. The subsequent qPCR was performed as described below. Immunoprecipitated samples were normalized to a 10% reverse crosslinked fraction of each chromatin preparation to calculate the percentage of input. Furthermore, the transcription start site region of the *ACT2* gene was used as a control for normalization in the HY5 ChIP experiment, while a negative region within the *FT* promoter was used in the CO ChIP experiment. Primers used to measure DNA fragments enriched during ChIP experiments are shown in Supplemental Table 9. Two biological replicates were processed for next-generation library preparation using the ThruPLEX DNA-seq kit (Takara). Next, libraries were sequenced on NextSeq500 (Illumina) at the Cabimer CSIC Genomics Unit. CO ChIP-seq analysis was implemented as described below. The raw data have been deposited in Gene Expression Omnibus (GEO: GSE222657).

ChIP-seq data acquisition and analysis

We used ChIP-seq data generated for TFs involved in flowering and the circadian clock that were available from the Sequence Read Archive, <https://www.ncbi.nlm.nih.gov/sra> (Wheeler et al., 2005). Specifically, data from 33 different TFs were downloaded in this study. These TFs and their ChIP-seq data accession numbers are shown in Supplemental Table 10. The *Arabidopsis* reference genome TAIR10 and its corresponding annotation were downloaded from the Ensembl Plants website (<http://plants.ensembl.org/index.html>). The FASTQC software package (v0.11.9) was employed to examine the read quality of each sample (<http://www.bioinformatics.babraham.ac.uk/projects/fastqc/>). The *fastq* files corresponding to each TF were mapped to the reference genome using the short-read mapper *bowtie* (v1.1.2) (Langmead et al., 2009). The read mappings for each sample were stored in SAM (Sequence Alignment Map, BAM (Binary Alignment Map), and *bigWig* files. We performed the “peak calling” step with the software tool MACS2 (2.2.9.1) (Zhang et al., 2008). Finally, target gene selection was carried out using *PeakAnnotator* (v1.3), part of the *PeakAnalyzer* program (Salmon-Divon et al., 2010), and an *ad hoc* R script developed in this study according to the criterion of the nearest downstream gene. DNA motif identification was carried out using *HOMER* software (v4.11) (Heinz et al., 2010). For further peak annotation and visualization, *ChIPseeker* (v1.30.3) (Yu et al., 2015) and *ChIPpeakAnno* (v3.28.1) (Zhu et al., 2010) R packages were employed. Finally, GO-term enrichment analysis was performed using the R package *clusterProfiler* (v4.2.2) (Wu et al., 2021). For the CO ChIP-seq analysis, peaks detected in the 35S:CO experiment were filtered based on the peaks found in *co-10* immunoprecipitation.

Transcriptional network construction and analysis

Our transcriptional network was generated and analyzed with the R package *igraph* (v1.6.0) (Csardi, 2006). Graphical representations of the network were done using *Cytoscape* (v3.10.1) (Smoot et al., 2011), a software package for network visualization and data integration.

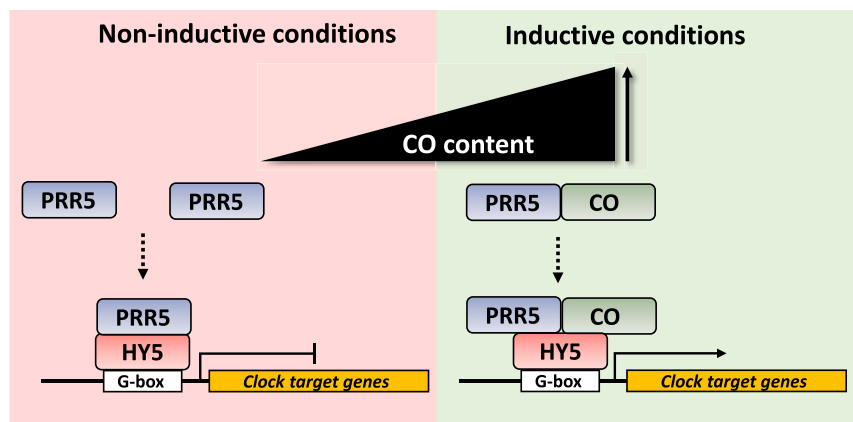


Figure 6. proposed model illustrating the possible mechanisms underlying the regulation of the circadian clock by CO.

Under non-inductive conditions, PRR5 binds to G boxes in the promoter of its target genes and represses their expression. When CO accumulates (in black density prism; i.e., LD), it binds to PRR5 to stabilize the complex and occupies the same genome-binding sites to activate the expression of its target genes. HY5 (or another bZIP TF) could mediate CO and PRR5 binding to the DNA.

Specifically, the “prefuse force layout” method was applied for network visualization. Additionally, a network topology analysis was achieved. The network node-degree distribution was calculated through degree function from the *igraph* package. To analyze if the network adjusts to the scale-free property, the power.law.fit function (*igraph* package) was used to test the node-degree distribution and determine whether it followed a power law. Furthermore, the network clustering coefficient and the average path length was calculated through transitivity and average-path.length functions, respectively. A network motif is a subgraph that appears a significantly higher number of times in the network of interest when compared to similar random networks. Therefore, we tested the significance of all possible subgraphs consisting of one, two, or three nodes by generating 100 000 random graphs with the same topological features as CircadianFloraTFNet. Network files and R scripts are available in <https://github.com/pedrodelosreyes/>.

RNA isolation and gene expression analysis

Total RNA from *Arabidopsis* seedlings (0.1 g of leaf tissue) was isolated by the TRIzol (Invitrogen) procedure following the recommendations of the manufacturer. The final RNA sample was suspended in 21 μ l of water, quantified in an ND-1000 spectrophotometer (Nanodrop), and stored at -80°C . Then, 500 ng of RNA was used to synthesize cDNA employing the QuantiTect Reverse Kit (Qiagen) and stored at -20°C until qPCR was performed. RT-qPCR was performed with the iQTM5 Multicolor Real-Time PCR Detection System (Bio-Rad) in 10- μ l reactions: primer concentration of 0.2 μ M, 10 ng of cDNA, and 5- μ l of SensiFAST SYBR & Fluorescein Kit (Bioline). Each sample was measured in triplicate. The RT-qPCR program consisted of (1) one cycle of 95°C for 2 min; (2) 40 cycles of 95°C for 5 s, 60°C for 10 s, and 72°C for 6 s; and (3) one cycle of 72°C for 6 s. Fluorescence was measured at the end of each extension step, and melting-curve analysis was performed between 55°C and 95°C . The initial concentrations were calculated using the ddCt Algorithm (Zhang et al., 2016). *UBQ10* expression was used as loading control. Primers used to measure gene expression by RT-qPCR are listed in Supplemental Table 9.

RNA-seq data acquisition and processing

In this study, we generated RNA-seq data and used other publicly available at the Sequence Read Archive. We analyzed different studies (GSE43865, GSE236178, and GSE205675) and obtained 31 samples representing four different genotypes, Col-0, *co-10*, SUC2:CO, and 35S:CO, under LD and LL conditions (see Supplemental Table 11). The quality control of each sample was carried out using the FASTQC software (v0.11.9), and the read sequences were mapped to the reference genome with the universal aligner STAR (v2.7.5b) (Dobin et al., 2013). The number of reads that mapped to each gene was performed using the *featureCounts* software of the *Subread* package (v2.0.1) (Liao et al., 2014). Genes with fewer than 10 counts per million in all samples were

removed, and TMM normalization and log2 transformation were performed with *calcNormFactors* (*edgeR* package v3.36.0; Robinson et al., 2010) and *voom* functions (*limma* package v3.50.3; Ritchie et al., 2015), respectively. Next, a linear model with the variable “genotype” was fitted for each gene using the *lmFit* function (*limma* package) in order to carry out the differential expression analyses. The differentially expressed genes were identified using a threshold of 1.5-fold change and an adjusted $p < 0.05$.

Protein analysis

Proteins were isolated from seedlings grown on MS-agar using a modification of the TRIzol (Invitrogen) protocol; separated by SDS-PAGE by standard procedures; transferred to nitrocellulose membranes; incubated with α CO, α GAPN (non-phosphorylating Glyceraldehyde-3-Phosphate Dehydrogenase) (Serrano-Bueno et al., 2020), or α HY5 (Agrisera); and developed with a chemiluminescent substrate (Clarity Western ECL, Bio-Rad). Blots were visualized and quantified in an Amersham Imager 680.

Determination of circadian genes and clustering techniques

The *bioconductor* R package *RAIN* (v1.38.0) (rhythmicity analysis incorporating non-parametric methods) (Thaben and Westermark, 2014) was used to determine diurnal genes, namely genes exhibiting rhythmic patterns of expression with a period of 24 h. A time interval of 4 h and a p value of 0.01 were used. Circadian genes were classified into clusters based on the positions of their peak (maximal level of expression) and trough (minimal level of expression) during a 24-h period.

Circadian leaf movement analysis

Plants were grown in LD until 7 DAG and then transferred to LL for six more days. The first pair of leaves was monitored using a Raspberry Pi camera. The leaf movement was tracked using *TRIP* software (v1.0) (Greenham et al., 2015) run in Octave (v9.1.0), and the vertical motion was obtained as a function of time and analyzed using *BioDare2* software (which performs FFT-NLLS period analysis) (Zielinski et al., 2014) and the *CircaCompare* package (v0.1.1) (Parsons et al., 2020) implemented in R. At least 12 plants were monitored in a minimum of two independent experiments. In the dexamethasone assay involving the 35S:CO:GR (*co-2*) line, six seedlings were analyzed in two separate experiments.

Transitory expression in *Nicotiana benthamiana*

To perform BiFC assays, CO, HY5, PRR5, and *FLM* cDNAs were cloned into pYFN43 and pYFC43 Gateway vectors (Belda-Palazón et al., 2012) producing an N-terminal fusion with nYFP and cYFP protein, respectively. Amino and carboxyl domains of AKIN β and AKIN10 sucrose-non-fermenting (Snf1)-related kinases were used as positive controls (Ferrando et al., 2001). *Agrobacterium tumefaciens* strain GVG3101 pmp90 were transformed with these constructs, and 4-week old *N. benthamiana* plants were infiltrated. Later, leaf disks were visualized with the Leica TCS SP2/DMRE confocal microscope. YFP was excited with the 514-nm line of an argon laser at 20% strength, and fluorescence

was detected between 515 and 565 nm. For ternary complex colocalization and FRET experiments, *HY5* and *PRR5* cDNAs were fused to C- and N-terminal fragments of YFP as in the BiFC assay, and *CO* and *FLM* cDNAs were cloned into pGWB644 and pGWB642 vectors, which produce a C-terminal fusion of full-length CFP and YFP, respectively (Shyu et al., 2008). CFP was excited with the 458 line under a Leica TCS SP2 confocal microscope, and the emission was detected between 465 and 479 nm. YFP was excited with a 514-nm laser, and the band-pass filters were adjusted to 520–545 nm. Colocalization was measured using the Pearson coefficient of correlation implemented in the *coloc2* plugin of the Fiji distribution of *ImageJ* (Schindelin et al., 2012).

Y2H assays

The DupLEX system was used to detect protein-protein interactions between CO domains and PRR5 or HY5. CO domains (CCT, middle, and B-box domains) were cloned into the bait vector pJG4-5, while full-length CDSs of *PRR5* or *HY5* were cloned into the prey vector pEG202. Primers used to generate Y2H clones are listed in Supplemental Table 9. EGY48 cells (MAT α *trp1 ura3 his3 LEU2::pLex Aop6-LEU2*) were used as the host strain for Y2H experiments (Gyuris et al., 1993). Single colonies grown on selection plates were inoculated in 3 ml of SD-Ura-His-Trp and grown overnight at 28°C. Saturated culture was then used to make serial dilutions with an optical density at 600 nm of 4⁻¹. Then, 2.5 μ l of the solution was then spotted on an SD-Ura-His-Trp plate, with an SGalRaf-Ura-His-Trp-Leu plate as a growth control. Plates were imaged after incubation for 60–72 h at 30°C.

Statistical analysis

The mean comparison between two sets of data was performed using the Student's *t*-test after testing the normality of the data with the Shapiro-Wilk test. The difference between means was considered statistically significant when the *p* value was less than 0.05 (marked with a single asterisk), 0.01 (marked with two asterisks), or 0.001 (marked with three asterisks). One-way ANOVA followed by Tukey's multiple comparisons test was employed to examine the mean differences among three or more groups. Fisher's exact test was used to analyze the significance of Venn diagram overlaps. Precisely, *shapiro.test*, *t.test*, *aov*, *TukeyHSD*, and *fisher.test* functions from R were employed. To determine the significance of overlapping peaks, Monte Carlo permutation tests were carried out, in which one of the peak sets was randomly shuffled and new intersections were calculated after each shuffle; 10 000 iterations were computed in order to estimate *p* values. These *p* values were corrected for multiple testing using the Benjamini-Hochberg method.

SUPPLEMENTAL INFORMATION

Supplemental information is available at *Molecular Plant Online*.

FUNDING

Work by G.S.-B. was supported by a European Union contract LONGFLOW, MSCAIF-2018- 838317 and CSIC LONGFLOW, CONV_EXT_014. The financial support of the Spanish Ministry for Science and Innovations (MICINN/FEDER) PID2020-117018RB-I00 to F.V. is also acknowledged. We thank Prof. George Coupland (MPIPZ, Cologne, Germany) for discussion and critical reading of the manuscript.

AUTHOR CONTRIBUTIONS

P.d.I.R., G.S.-B., F.J.R.-C., J.M.R. and F.V. designed the experimental approach. P.d.I.R., G.S.-B., H.G., and F.V. performed most experiments. P.d.I.R. and F.J.R.-C. provided the RNA-seq analysis. P.d.I.R., G.S.-B., J.M.R., and F.V. wrote the paper. J.M.R., F.J.R.-C. and F.V. supervised work. The final version of the manuscript was reviewed and revised by all authors.

ACKNOWLEDGMENTS

No conflict of interest is declared.

Received: July 19, 2023

Revised: April 23, 2024

Accepted: June 11, 2024

Published: June 17, 2024

REFERENCES

- Abbas, N., Maurya, J.P., Senapati, D., Gangappa, S.N., and Chattopadhyay, S. (2014). *Arabidopsis* CAM7 and HY5 physically interact and directly bind to the HY5 promoter to regulate its expression and thereby promote photomorphogenesis. *Plant Cell* **26**:1036–1052.
- An, H., Roussot, C., Suárez-López, P., Corbesier, L., Vincent, C., Piñeiro, M., Hepworth, S., Mouradov, A., Justin, S., Turnbull, C., and Coupland, G. (2004). CONSTANS acts in the phloem to regulate a systemic signal that induces photoperiodic flowering of *Arabidopsis*. *Development* **131**:3615–3626.
- Ando, E., Ohnishi, M., Wang, Y., Matsushita, T., Watanabe, A., Hayashi, Y., Fujii, M., Ma, J.F., Inoue, S.I., and Kinoshita, T. (2013). TWIN SISTER OF FT, GIGANTEA, and CONSTANS have a positive but indirect effect on blue light-induced stomatal opening in *Arabidopsis*. *Plant Physiol.* **162**:1529–1538.
- Andrés, F., and Coupland, G. (2012). The genetic basis of flowering responses to seasonal cues. *Nat. Rev. Genet.* **13**:627–639.
- Barabási, A.-L. (2015). *Network Science*.
- Belda-Palazón, B., Ruiz, L., Martí, E., Tárrega, S., Tiburcio, A.F., Culiñez, F., Farràs, R., Carrasco, P., and Ferrando, A. (2012). Aminopropyltransferases Involved in Polyamine Biosynthesis Localize Preferentially in the Nucleus of Plant Cells. *PLoS One* **7**:e46907.
- Bhagat, P.K., Verma, D., Sharma, D., and Sinha, A.K. (2021). HY5 and ABI5 transcription factors physically interact to fine tune light and ABA signaling in *Arabidopsis*. *Plant Mol. Biol.* **107**:117–127.
- Binkert, M., Kozma-Bognár, L., Terecskei, K., De Veylder, L., Nagy, F., and Ulm, R. (2014). UV-B-Responsive association of the *Arabidopsis* bZIP transcription factor ELONGATED HYPOCOTYL5 with target genes, including its own promoter. *Plant Cell* **26**:4200–4213.
- Blackman, B.K., and Michaels, S.D. (2010). Does CONSTANS act as a transcription factor or as a co-activator? The answer may be - yes. *New Phytol.* **187**:1–3.
- Bowler, C., Benvenuto, G., Laflamme, P., Molino, D., Probst, A.V., Tariq, M., and Paszkowski, J. (2004). Chromatin techniques for plant cells. *Plant J.* **39**:776–789.
- Bursch, K., Toledo-Ortiz, G., Pireyre, M., Lohr, M., Braatz, C., and Johansson, H. (2020). Identification of BBX proteins as rate-limiting cofactors of HY5. *Nat. Plants* **6**:921–928.
- Chattopadhyay, S., Ang, L.H., Puente, P., Deng, X.W., and Wei, N. (1998). *Arabidopsis* bZIP protein HY5 directly interacts with light-responsive promoters in mediating light control of gene expression. *Plant Cell* **10**:673–683.
- Csardi, G.N.T. (2006). The igraph software package for complex network research. *Inter J Complex Syst* **1695**.
- Datta, S., Hettiarachchi, C., Johansson, H., and Holm, M. (2007). SALT TOLERANCE HOMOLOG2, a B-Box Protein in *Arabidopsis* That Activates Transcription and Positively Regulates Light-Mediated Development. *Plant Cell* **19**:3242–3255.
- de los Reyes, P., Romero-Campero, F.J., Ruiz, M.T., Romero, J.M., and Valverde, F. (2017). Evolution of daily gene co-expression patterns from algae to plants. *Front. Plant Sci.* **8**:1217.
- De Mendoza, A., Sebé-Pedrós, A., Šestak, M.S., Matejčić, M., Torruella, G., Domazet-Lošo, T., and Ruiz-Trillo, I. (2013). Transcription factor evolution in eukaryotes and the assembly of the

- regulatory toolkit in multicellular lineages. *Proc. Natl. Acad. Sci. USA* **110**:E4858–E4866.
- Dobin, A., Davis, C.A., Schlesinger, F., Drenkow, J., Zaleski, C., Jha, S., Batut, P., Chaisson, M., and Gingeras, T.R.** (2013). STAR: ultrafast universal RNA-seq aligner. *Bioinformatics* **29**:15–21.
- Endo, M., Tanigawa, Y., Murakami, T., Araki, T., and Nagatani, A.** (2013). Phytochrome-dependent late-flowering accelerates flowering through physical interactions with phytochrome B and CONSTANS. *Proc. Natl. Acad. Sci. USA* **110**:18017–18022.
- Endo, M., Shimizu, H., Nohales, M.A., Araki, T., and Kay, S.A.** (2014). Tissue-specific clocks in *Arabidopsis* show asymmetric coupling. *Nature* **515**:419–422.
- Fernández, V., Takahashi, Y., Le Gourrierc, J., and Coupland, G.** (2016). Photoperiodic and thermosensory pathways interact through CONSTANS to promote flowering at high temperature under short days. *Plant J.* **86**:426–440.
- Ferrando, A., Koncz-Kálmán, Z., Farràs, R., Tiburcio, A., Schell, J., and Koncz, C.** (2001). Detection of in vivo protein interactions between Snf1-related kinase subunits with intron-tagged epitope-labelling in plants cells. *Nucleic Acids Res.* **29**:3685–3693.
- Gangappa, S.N., and Botto, J.F.** (2016). The Multifaceted Roles of HY5 in Plant Growth and Development. *Mol. Plant* **9**:1353–1365.
- Gnesutta, N., Kumimoto, R.W., Swain, S., Chiara, M., Siriwardana, C., Horner, D.S., Holt, B.F., and Mantovani, R.** (2017). CONSTANS imparts DNA sequence specificity to the histone fold NF-YB/NF-YC Dimer. *Plant Cell* **29**:1516–1532.
- Goldstein, M.L., Morris, S.A., and Yen, G.G.** (2004). Problems with fitting to the power-law distribution. *Eur. Phys. J. B* **41**:255–258.
- Graeff, M., Straub, D., Eguen, T., Dolde, U., Rodrigues, V., Brandt, R., and Wenkel, S.** (2016). MicroProtein-Mediated Recruitment of CONSTANS into a TOPLESS Trimeric Complex Represses Flowering in *Arabidopsis*. *PLoS Genet.* **12**:e1005959.
- Greenham, K., Lou, P., Remsen, S.E., Farid, H., and McClung, C.R.** (2015). TRiP: Tracking Rhythms in Plants, an automated leaf movement analysis program for circadian period estimation. *Plant Methods* **11**:33.
- Gyuris, J., Golemis, E., Chertkov, H., and Brent, R.** (1993). Cdi1, a human G1 and S phase protein phosphatase that associates with Cdk2. *Cell* **75**:791–803.
- Hajdu, A., Ádám, É., Sheerin, D.J., Dobos, O., Bernula, P., Hiltbrunner, A., Kozma-Bognár, L., and Nagy, F.** (2015). High-level expression and phosphorylation of phytochrome B modulates flowering time in *Arabidopsis*. *Plant J.* **83**:794–805.
- Hajdu, A., Dobos, O., Domijan, M., Bálint, B., Nagy, I., Nagy, F., and Kozma-Bognár, L.** (2018). ELONGATED HYPOCOTYL 5 mediates blue light signalling to the *Arabidopsis* circadian clock. *Plant J.* **96**:1242–1254.
- Harmer, S.L., and Kay, S.A.** (2005). Positive and Negative Factors Confer Phase-Specific Circadian Regulation of Transcription in *Arabidopsis*. *Plant Cell* **17**:1926–1940.
- Hayama, R., Sarid-Krebs, L., Richter, R., Fernández, V., Jang, S., and Coupland, G.** (2017). PSEUDO RESPONSE REGULATORS stabilize CONSTANS protein to promote flowering in response to day length. *EMBO J.* **36**:904–918.
- Heinz, S., Benner, C., Spann, N., Bertolino, E., Lin, Y.C., Laslo, P., Cheng, J.X., Murre, C., Singh, H., and Glass, C.K.** (2010). Simple combinations of lineage-determining transcription factors prime cis-regulatory elements required for macrophage and B cell identities. *Mol. Cell* **38**:576–589.
- Huang, W., Pérez-García, P., Pokhilko, A., Millar, A.J., Antoshechkin, I., Riechmann, J.L., and Mas, P.** (2012). Mapping the core of the *Arabidopsis* circadian clock defines the network structure of the oscillator. *Science* **335**:75–79.
- Imaizumi, T., Schultz, T.F., Harmon, F.G., Ho, L.A., and Kay, S.A.** (2005). Plant science: FKF1 F-box protein mediates cyclic degradation of a repressor of CONSTANS in *Arabidopsis*. *Science* **309**:293–297.
- Ito, S., Song, Y.H., Josephson-Day, A.R., Miller, R.J., Breton, G., Olmstead, R.G., and Imaizumi, T.** (2012). FLOWERING BHLH transcriptional activators control expression of the photoperiodic flowering regulator CONSTANS in *Arabidopsis*. *Proc. Natl. Acad. Sci. USA* **109**:3582–3587.
- Jang, S., Marchal, V., Panigrahi, K.C.S., Wenkel, S., Soppe, W., Deng, X.W., Valverde, F., and Coupland, G.** (2008). *Arabidopsis* COP1 shapes the temporal pattern of CO accumulation conferring a photoperiodic flowering response. *EMBO J.* **27**:1277–1288.
- Jing, Y., Zhang, D., Wang, X., Tang, W., Wang, W., Huai, J., Xu, G., Chen, D., Li, Y., and Lin, R.** (2013). *Arabidopsis* chromatin remodeling factor PICKLE interacts with transcription factor HY5 to regulate hypocotyl cell elongation. *Plant Cell* **25**:242–256.
- Jing, Y., Guo, Q., Zha, P., and Lin, R.** (2019). The chromatin-remodelling factor PICKLE interacts with CONSTANS to promote flowering in *Arabidopsis*. *Plant Cell Environ.* **42**:2495–2507.
- Job, N., Yadukrishnan, P., Bursch, K., Datta, S., and Johansson, H.** (2018). Two B-Box Proteins Regulate Photomorphogenesis by Oppositely Modulating HY5 through their Diverse C-Terminal Domains. *Plant Physiol.* **176**:2963–2976.
- Kinoshita, A., and Richter, R.** (2020). Genetic and molecular basis of floral induction in *Arabidopsis thaliana*. *J. Exp. Bot.* **71**:2490–2504.
- Langmead, B., Trapnell, C., Pop, M., and Salzberg, S.L.** (2009). Ultrafast and memory-efficient alignment of short DNA sequences to the human genome. *Genome Biol.* **10**:R25.
- Lau, O.S., and Bergmann, D.C.** (2015). MOBE-ChIP: a large-scale chromatin immunoprecipitation assay for cell type-specific studies. *Plant J.* **84**:443–450.
- Laubinger, S., Marchal, V., Le Gourrierc, J., Wenkel, S., Adrian, J., Jang, S., Kulajta, C., Braun, H., Coupland, G., and Hoecker, U.** (2006). *Arabidopsis* SPA proteins regulate photoperiodic flowering and interact with the floral inducer CONSTANS to regulate its stability. *Development* **133**:3213–3222.
- Lazaro, A., Valverde, F., Piñeiro, M., and Jarillo, J.A.** (2012). The *Arabidopsis* E3 ubiquitin ligase HOS1 negatively regulates CONSTANS abundance in the photoperiodic control of flowering. *Plant Cell* **24**:982–999.
- Lazaro, A., Mouriz, A., Piñeiro, M., and Jarillo, J.A.** (2015). Red Light-Mediated Degradation of CONSTANS by the E3 Ubiquitin Ligase HOS1 Regulates Photoperiodic Flowering in *Arabidopsis*. *Plant Cell* **27**:2437–2454.
- Ledger, S., Strayer, C., Ashton, F., Kay, S.A., and Putterill, J.** (2001). Analysis of the function of two circadian-regulated CONSTANS-LIKE genes. *Plant J.* **26**:15–22.
- Lee, J., He, K., Stolc, V., Lee, H., Figueroa, P., Gao, Y., Tongprasit, W., Zhao, H., Lee, I., and Deng, X.W.** (2007). Analysis of transcription factor HY5 genomic binding sites revealed its hierarchical role in light regulation of development. *Plant Cell* **19**:731–749.
- Li, N., Zhang, Y., He, Y., Wang, Y., and Wang, L.** (2020). Pseudo Response Regulators regulate photoperiodic hypocotyl growth by repressing PIF4/5 transcription. *Plant Physiol.* **183**:686–699. <https://doi.org/10.1104/pp.19.01599>.
- Liao, Y., Smyth, G.K., and Shi, W.** (2014). featureCounts: an efficient general purpose program for assigning sequence reads to genomic features. *Bioinformatics* **30**:923–930.

- Liu, L.J., Zhang, Y.C., Li, Q.H., Sang, Y., Mao, J., Lian, H.L., Wang, L., and Yang, H.Q. (2008). COP1-mediated ubiquitination of CONSTANS is implicated in cryptochrome regulation of flowering in *Arabidopsis*. *Plant Cell* **20**:292–306.
- Liu, B., Zuo, Z., Liu, H., Liu, X., and Lin, C. (2011). *Arabidopsis* cryptochrome 1 interacts with SPA1 to suppress COP1 activity in response to blue light. *Genes Dev.* **25**:1029–1034.
- Liu, T., Carlsson, J., Takeuchi, T., Newton, L., and Farré, E.M. (2013a). Direct regulation of abiotic responses by the *Arabidopsis* circadian clock component PRR7. *Plant J.* **76**:101–114.
- Liu, Y., Li, X., Li, K., Liu, H., and Lin, C. (2013b). Multiple bHLH Proteins form Heterodimers to Mediate CRY2-Dependent Regulation of Flowering-Time in *Arabidopsis*. *PLoS Genet.* **9**:e1003861.
- Liu, T.L., Newton, L., Liu, M.-J., Shiu, S.-H., and Farré, E.M. (2016). A G-Box-Like Motif Is Necessary for Transcriptional Regulation by Circadian Pseudo-Response Regulators in *Arabidopsis*. *Plant Physiol.* **170**:528–539.
- Martín, G., Rovira, A., Veciana, N., Soy, J., Toledo-Ortiz, G., Gommers, C.M.M., Boix, M., Henriques, R., Minguet, E.G., Alabadi, D., et al. (2018). Circadian Waves of Transcriptional Repression Shape PIF-Regulated Photoperiod-Responsive Growth in *Arabidopsis*. *Curr. Biol.* **28**:311–318.e5.
- McClung, C.R. (2006). Plant circadian rhythms. *Plant Cell* **18**:792–803.
- McClung, C.R. (2014). Wheels within wheels: New transcriptional feedback loops in the *Arabidopsis* circadian clock. *F1000Prime Rep.* **6**:2.
- Mellis, I.A., and Raj, A. (2015). Half dozen of one, six billion of the other: What can small- and large-scale molecular systems biology learn from one another? *Genome Res.* **25**:1466–1472.
- Michael, T.P., Salomé, P.A., Yu, H.J., Spencer, T.R., Sharp, E.L., McPeck, M.A., Alonso, J.M., Ecker, J.R., and McClung, C.R. (2003). Enhanced Fitness Conferred by Naturally Occurring Variation in the Circadian Clock. *Science* **302**:1049–1053.
- Michael, T.P., Mockler, T.C., Breton, G., McEntee, C., Byer, A., Trout, J.D., Hazen, S.P., Shen, R., Priest, H.D., Sullivan, C.M., et al. (2008). Network Discovery Pipeline Elucidates Conserved Time-of-Day-Specific cis-Regulatory Modules. *PLoS Genet.* **4**:e14.
- Milo, R., Shen-Orr, S., Itzkovitz, S., Kashtan, N., Chklovskii, D., and Alon, U. (2002). Network motifs: Simple building blocks of complex networks. *Science* **298**:824–827.
- Mizoguchi, T., Wright, L., Fujiwara, S., Cremer, F., Lee, K., Onouchi, H., Mouradov, A., Fowler, S., Kamada, H., Putterill, J., and Coupland, G. (2005). Distinct roles of GIGANTEA in promoting flowering and regulating circadian rhythms in *Arabidopsis*. *Plant Cell* **17**:2255–2270.
- Nakamichi, N., Kita, M., Niinuma, K., Ito, S., Yamashino, T., Mizoguchi, T., and Mizuno, T. (2007). *Arabidopsis* Clock-Associated Pseudo-Response Regulators PRR9, PRR7 and PRR5 Coordinately and Positively Regulate Flowering Time Through the Canonical CONSTANS-Dependent Photoperiodic Pathway. *Plant Cell Physiol.* **48**:822–832.
- Nakamichi, N., Kiba, T., Henriques, R., Mizuno, T., Chua, N.-H., and Sakakibara, H. (2010). PSEUDO-RESPONSE REGULATORS 9, 7, and 5 are transcriptional repressors in the *Arabidopsis* circadian clock. *Plant Cell* **22**:594–605.
- Nakamichi, N., Kiba, T., Kamioka, M., Suzuki, T., Yamashino, T., Higashiyama, T., Sakakibara, H., and Mizuno, T. (2012). Transcriptional repressor PRR5 directly regulates clock-output pathways. *Proc. Natl. Acad. Sci. USA* **109**:17123–17128.
- Nguyen, K.T., Park, J., Park, E., Lee, I., and Choi, G. (2015). The *Arabidopsis* RING Domain Protein BOI Inhibits Flowering via CO-dependent and CO-independent Mechanisms. *Mol. Plant* **8**:1725–1736.
- Onouchi, H., Igeño, M.I., Périlleux, C., Graves, K., and Coupland, G. (2000). Mutagenesis of Plants Overexpressing CONSTANS Demonstrates Novel Interactions among *Arabidopsis* Flowering-Time Genes. *Plant Cell* **12**:885–900.
- Ortiz-Marchena, M.I., Albi, T., Lucas-Reina, E., Said, F.E., Romero-Campero, F.J., Cano, B., Ruiz, M.T., Romero, J.M., and Valverde, F. (2014). Photoperiodic control of carbon distribution during the floral transition in *Arabidopsis*. *Plant Cell* **26**:565–584.
- Osterlund, M.T., Hardtke, C.S., Wei, N., and Deng, X.W. (2000). Targeted destabilization of HY5 during light-regulated development of *Arabidopsis*. *Nature* **405**:462–466.
- Parsons, R., Parsons, R., Garner, N., Oster, H., and Rawashdeh, O. (2020). CircaCompare: A method to estimate and statistically support differences in mesor, amplitude and phase, between circadian rhythms. *Bioinformatics* **36**:1208–1212.
- Piñeiro, M., and Jarillo, J.A. (2013). Ubiquitination in the control of photoperiodic flowering. *Plant Sci.* **198**:98–109.
- Putterill, J., Robson, F., Lee, K., Simon, R., and Coupland, G. (1995). The CONSTANS gene of *Arabidopsis* promotes flowering and encodes a protein showing similarities to zinc finger transcription factors. *Cell* **80**:847–857.
- Qin, Y., Liu, Z., Gao, S., Long, Y., Zhu, X., Liu, B., Gao, Y., Xie, Q., Nohales, M.A., Xu, X., et al. (2023). A Day in the Life of *Arabidopsis*: 24-Hour Time-lapse Single-nucleus Transcriptomics Reveal Cell-type specific Circadian Rhythms. Preprint at bioRxiv. <https://doi.org/10.1101/2023.12.09.570919>.
- Ritchie, M.E., Phipson, B., Wu, D., Hu, Y., Law, C.W., Shi, W., and Smyth, G.K. (2015). limma powers differential expression analyses for RNA-sequencing and microarray studies. *Nucleic Acids Res.* **43**:e47.
- Robinson, M.D., McCarthy, D.J., and Smyth, G.K. (2010). edgeR: a Bioconductor package for differential expression analysis of digital gene expression data. *Bioinformatics* **26**:139–140.
- Romero, J.M., and Valverde, F. (2009). Evolutionarily conserved photoperiod mechanisms in plants: When did plant photoperiodic signaling appear? *Plant Signal. Behav.* **4**:642–644.
- Romero-Campero, F.J., Lucas-Reina, E., Said, F.E., Romero, J.M., and Valverde, F. (2013). A contribution to the study of plant development evolution based on gene co-expression networks. *Front. Plant Sci.* **4**:291.
- Rugnone, M.L., Faigón Soverna, A., Sanchez, S.E., Schlaen, R.G., Hernando, C.E., Seymour, D.K., Mancini, E., Chernomoretz, A., Weigel, D., Más, P., and Yanovsky, M.J. (2013). LNK genes integrate light and clock signaling networks at the core of the *Arabidopsis* oscillator. *Proc. Natl. Acad. Sci. USA* **110**:12120–12125.
- Salmon-Divon, M., Dvinge, H., Tammoja, K., and Bertone, P. (2010). PeakAnalyzer: Genome-wide annotation of chromatin binding and modification loci. *BMC Bioinf.* **11**:415.
- Sanchez, S.E., and Kay, S.A. (2016). The Plant Circadian Clock: From a Simple Timekeeper to a Complex Developmental Manager. *Cold Spring Harbor Perspect. Biol.* **8**:a027748.
- Sawa, M., Nusinow, D.A., Kay, S.A., and Imaizumi, T. (2007). FKF1 and GIGANTEA complex formation is required for day-length measurement in *Arabidopsis*. *Science* **318**:261–265.
- Schindelin, J., Arganda-Carreras, I., Frise, E., Kaynig, V., Longair, M., Pietzsch, T., Preibisch, S., Rueden, C., Saalfeld, S., Schmid, B., et al. (2012). Fiji: An open-source platform for biological-image analysis. *Nat. Methods* **9**:676–682.

- Serrano-Bueno, G., Said, F.E., de Los Reyes, P., Lucas-Reina, E.I., Ortiz-Marchena, M.I., Romero, J.M., and Valverde, F. (2020). CONSTANS-FKBP12 interaction contributes to modulation of photoperiodic flowering in *Arabidopsis*. *Plant J.* **101**:1287–1302.
- Serrano-Bueno, G., Sánchez de Medina Hernández, V., and Valverde, F. (2021). Photoperiodic Signaling and Senescence, an Ancient Solution to a Modern Problem? *Front. Plant Sci.* **12**:634393.
- Serrano-Bueno, G., de los Reyes, P., Chini, A., Ferreras-Garrucho, G., Sánchez de Medina-Hernández, V., Boter, M., Solano, R., and Valverde, F. (2022). Regulation of floral senescence in *Arabidopsis* by coordinated action of CONSTANS and jasmonate signaling. *Mol. Plant* **15**:1710–1724. <https://doi.org/10.1016/j.molp.2022.09.017>.
- Sheerin, D.J., Menon, C., zur Oven-Krockhaus, S., Enderle, B., Zhu, L., Johnen, P., Schleifenbaum, F., Stierhof, Y.D., Huq, E., and Hiltbrunner, A. (2015). Light-activated phytochrome A and B interact with members of the SPA family to promote photomorphogenesis in *Arabidopsis* by reorganizing the COP1/SPA complex. *Plant Cell* **27**:189–201.
- Shen, C., Liu, H., Guan, Z., Yan, J., Zheng, T., Yan, W., Wu, C., Zhang, Q., Yin, P., and Xing, Y. (2020). Structural Insight into DNA Recognition by CCT/NF-YB/YC Complexes in Plant Photoperiodic Flowering. *Plant Cell* **32**:3469–3484.
- Shen-Orr, S.S., Milo, R., Mangan, S., and Alon, U. (2002). Network motifs in the transcriptional regulation network of *Escherichia coli*. *Nat. Genet.* **31**:64–68.
- Shim, J.S., Kubota, A., and Imaizumi, T. (2017). Circadian clock and photoperiodic flowering in *Arabidopsis*: CONSTANS is a Hub for Signal integration. *Plant Physiol.* **173**:5–15.
- Shyu, Y.J., Suarez, C.D., and Hu, C.D. (2008). Visualization of ternary complexes in living cells by using a BiFC-based FRET assay. *Nat. Protoc.* **3**:1693–1702.
- Simon, R., Igeño, M.I., and Coupland, G. (1996). Activation of floral meristem identity genes in *Arabidopsis*. *Nature* **384**:59–62.
- Smoot, M.E., Ono, K., Ruscheinski, J., Wang, P.-L., and Ideker, T. (2011). Cytoscape 2.8: new features for data integration and network visualization. *Bioinformatics England* **27**:431–432.
- Song, Y.H., Smith, R.W., To, B.J., Millar, A.J., and Imaizumi, T. (2012). FKF1 conveys timing information for CONSTANS stabilization in photoperiodic flowering. *Science* **336**:1045–1049.
- Song, Y.H., Estrada, D.A., Johnson, R.S., Kim, S.K., Lee, S.Y., MacCoss, M.J., and Imaizumi, T. (2014). Distinct roles of FKF1, GIGANTEA, and ZEITLUPE proteins in the regulation of constans stability in *Arabidopsis* photoperiodic flowering. *Proc. Natl. Acad. Sci. USA* **111**:17672–17677.
- Stone, L., Simberloff, D., and Artzy-Randrup, Y. (2019). Network motifs and their origins. *PLoS Comput. Biol.* **15**:e1006749.
- Strayer, C., Oyama, T., Schultz, T.F., Raman, R., Somers, D.E., Más, P., Panda, S., Kreps, J.A., and Kay, S.A. (2000). Cloning of the *Arabidopsis* clock gene *TOC1*, an autoregulatory response regulator homolog. *Science* **289**:768–771.
- Suárez-López, P., Wheatley, K., Robson, F., Onouchi, H., Valverde, F., and Coupland, G. (2001). CONSTANS mediates between the circadian clock and the control of flowering in *Arabidopsis*. *Nature* **410**:1116–1120.
- Thaben, P.F., and Westermark, P.O. (2014). Detecting rhythms in time series with RAIN. *J. Biol. Rhythms* **29**:391–400.
- Tiwari, S.B., Shen, Y., Chang, H.-C., Hou, Y., Harris, A., Ma, S.F., McPartland, M., Hymus, G.J., Adam, L., Marion, C., et al. (2010). The flowering time regulator CONSTANS is recruited to the FLOWERING LOCUS T promoter via a unique cis-element. *New Phytol.* **187**:57–66.
- Tong, A.H.Y., Lesage, G., Bader, G.D., Ding, H., Xu, H., Xin, X., Young, J., Berriz, G.F., Brost, R.L., Chang, M., et al. (2004). Global Mapping of the Yeast Genetic Interaction Network. *Science* **303**:808–813.
- Valverde, F. (2011). CONSTANS and the evolutionary origin of photoperiodic timing of flowering. *J. Exp. Bot.* **62**:2453–2463.
- Valverde, F., Mouradov, A., Soppe, W., Ravenscroft, D., Samach, A., and Coupland, G. (2004). Photoreceptor Regulation of CONSTANS Protein in Photoperiodic Flowering. *Science* **303**:1003–1006.
- Wagner, A., and Fell, D.A. (2001). The small world inside large metabolic networks. *Proc. Biol. Sci.* **268**:1803–1810.
- Wang, Z.Y., and Tobin, E.M. (1998). Constitutive expression of the *CIRCADIAN CLOCK ASSOCIATED 1 (CCA1)* gene disrupts circadian rhythms and suppresses its own expression. *Cell* **93**:1207–1217.
- Wang, C.Q., Guthrie, C., Sarmast, M.K., and Dehesh, K. (2014). BBX19 interacts with CONSTANS to repress FLOWERING LOCUS T transcription, defining a flowering time checkpoint in *Arabidopsis*. *Plant Cell* **26**:3589–3602.
- Wang, H., Pan, J., Li, Y., Lou, D., Hu, Y., and Yu, D. (2016). The DELLA-CONSTANS transcription factor cascade integrates gibberellic acid and photoperiod signaling to regulate flowering. *Plant Physiol.* **172**:479–488.
- Wenkel, S., Turck, F., Singer, K., Gissot, L., Le Gourrierec, J., Samach, A., and Coupland, G. (2006). CONSTANS and the CCAAT box binding complex share a functionally important domain and interact to regulate flowering of *Arabidopsis*. *Plant Cell* **18**:2971–2984.
- Wheeler, D.L., Barrett, T., Benson, D.A., Bryant, S.H., Canese, K., Church, D.M., DiCuccio, M., Edgar, R., Federhen, S., Helmsberg, W., et al. (2005). Database resources of the National Center for Biotechnology Information. *Nucleic Acids Res.* **33**:D39–D45.
- Wu, T., Hu, E., Xu, S., Chen, M., Guo, P., Dai, Z., Feng, T., Zhou, L., Tang, W., Zhan, L., et al. (2021). clusterProfiler 4.0: A universal enrichment tool for interpreting omics data. *Innovation* **2**:100141.
- Xu, F., Li, T., Xu, P.-B., Li, L., Du, S.-S., Lian, H.-L., and Yang, H.-Q. (2016). DELLA proteins physically interact with CONSTANS to regulate flowering under long days in *Arabidopsis*. *FEBS Lett.* **590**:541–549.
- Yanovsky, M.J., and Kay, S.A. (2002). Molecular basis of seasonal time measurement in *Arabidopsis*. *Nature* **419**:308–312.
- Yook, S.-H., Oltvai, Z.N., and Barabási, A.-L. (2004). Functional and topological characterization of protein interaction networks. *Proteomics* **4**:928–942.
- Young, H.S., Cheol, M.Y., An, P.H., Seong, H.K., Hee, J.J., Su, Y.S., Hye, J.K., Yun, D.J., Chae, O.L., Jeong, D.B., et al. (2008). DNA-binding study identifies C-box and hybrid C/G-box or C/A-box motifs as high-affinity binding sites for STF1 and long hypocotyl5 proteins. *Plant Physiology* **146**:1862–1877.
- Yu, G., Wang, L.-G., and He, Q.-Y. (2015). ChIPseeker: an R/Bioconductor package for ChIP peak annotation, comparison and visualization. *Bioinformatics* **31**:2382–2383.
- Yu, Y., Su, C., He, Y., and Wang, L. (2023a). B-Box proteins BBX28 and BBX29 interplay with PSEUDO-RESPONSE REGULATORS to fine-tune circadian clock in *Arabidopsis*. *Plant Cell Environ.* **46**:2810–2826.
- Yu, B., He, X., Tang, Y., Chen, Z., Zhou, L., Li, X., Zhang, C., Huang, X., Yang, Y., Zhang, W., et al. (2023b). Photoperiod controls plant seed size in a CONSTANS-dependent manner. *Nat. Plants* **9**:343–354.
- Yuan, L., Yu, Y., Liu, M., Song, Y., Li, H., Sun, J., Wang, Q., Xie, Q., Wang, L., and Xu, X. (2021). BBX19 fine-tunes the circadian rhythm by interacting with PSEUDO-RESPONSE REGULATOR proteins to facilitate their repressive effect on morning-phased clock genes. *Plant Cell* **33**:2602–2617.

Molecular Plant

- Zhang, Y., Liu, T., Meyer, C.A., Eeckhoute, J., Johnson, D.S., Bernstein, B.E., Nusbaum, C., Myers, R.M., Brown, M., Li, W., and Liu, X.S.** (2008). Model-based analysis of ChIP-Seq (MACS). *Genome Biol.* **9**:R137.
- Zhang, H., He, H., Wang, X., Wang, X., Yang, X., Li, L., and Deng, X.W.** (2011). Genome-wide mapping of the HY5-mediated gene networks in *Arabidopsis* that involve both transcriptional and post-transcriptional regulation. *Plant J.* **65**:346–358.
- Zhang, J.D., Ruschhaupt, M., and Biczok, R.** (2016). ddCt method for qRT-PCR data analysis. *Citeseer* **48**:346–356.
- Zhu, L.J., Gazin, C., Lawson, N.D., Pagès, H., Lin, S.M., Lapointe, D.S., and Green, M.R.** (2010). ChIPpeakAnno: a Bioconductor package to annotate ChIP-seq and ChIP-chip data. *BMC Bioinf.* **11**:237.
- Zielinski, T., Moore, A.M., Troup, E., Halliday, K.J., and Millar, A.J.** (2014). Strengths and Limitations of Period Estimation Methods for Circadian Data. *PLoS One* **9**:e96462.
- Zuo, Z., Liu, H., Liu, B., Liu, X., and Lin, C.** (2011). Blue light-dependent interaction of CRY2 with SPA1 regulates COP1 activity and floral initiation in *Arabidopsis*. *Curr. Biol.* **21**:841–847.

Control of *Arabidopsis* clock by CONSTANS